An-Najah National University

Faculty of Graduate Studies

DOWN-REGULATION OF BETA-CATENIN IN CANCER CELLS BY SIRNA COMPLEXED WITH CARBON NANOTUBE

By

Ahmad Ghareeb

Supervisors

Dr. Naim Kittana

Dr. Mohyeddin Assali

This Thesis is Submitted in Partial Fulfillment of the Requirements for the Degree of Master of Pharmacology, Faculty of Graduate Studies, An-Najah National University, Nablus - Palestine.

2023

DOWN-REGULATION OF BETA-CATENIN IN CANCER CELLS BY SIRNA COMPLEXED WITH CARBON NANOTUBE

By

Ahmad Ghareeb

This Thesis was Defended Successfully on 14/3/2023 and approved by

Dr. Naim Kittana Supervisor	Signature
Dr. Mohyeddin Assali Co-Supervisor	Signature
Dr. Abdullah Rabba External Examiner	Signature
Dr. Ahmed Eid Internal Examiner	Signature

Dedication

I dedicate this dissertation to Allah Almighty, my source of strength, inspiration, wisdom, and knowledge. I also dedicate this work to my parents, and siblings, who have motivated me during my master's studies. Additionally, I dedicate this thesis to all my friends and anyone who assisted when needed to tackle any task enthusiastically and persistently. Furthermore, I specially dedicate this thesis to my beloved passed-away father, who dreamt to see me one day as a pioneer in my profession.

Acknowledgements

First and foremost, I am thankful to the holy god for giving me the strength, ability, and patience to successfully complete this prestigious research.

Secondly, my deepest appreciation and thanks go to those who deserve the utmost credit, my dear supervisors, Dr. Mohyeddin Assali and Dr. Naim Kittana for everything I learned from their valuable experience during these years and the memories that will last forever.

I would also like to thank the respectful examination committee, who critiqued my thesis, offered insightful comments and suggestions, and provided valuable feedback.

Moreover, thanks go to the laboratory staff at the Pharmacy, Sciences, and Medicine faculties for their endless assistance and support.

Let me also share my heartfelt thanks to my friends and colleagues. Thanks to their guidance, support, and the most joyful memories we shared, I reached this milestone in my life.

Finally, and most importantly, no words can describe my happiness at making my family proud. I would never forget the love, support, and gratitude they have given me throughout my years of study and research.

Declaration

I, the undersigned, declare that I submitted the thesis entitled:

DOWN-REGULATION OF BETA-CATENIN IN CANCER CELLS BY SIRNA COMPLEXED WITH CARBON NANOTUBE

I declare that the work provided in this thesis, unless otherwise referenced, is the researcher's own work, and has not been submitted elsewhere for any other degree or qualification.

Student's Name: _____

Signature: _____

Date: 14-3-2023

List of Contents

List of Tables

List of Figures

List of Scheme

DOWN-REGULATION OF BETA-CATENIN IN CANCER CELLS BY SIRNA COMPLEXED WITH CARBON NANOTUBE

By
Ahmad Ghareeb
Supervisors
Dr. Naim Kittana
Dr. Mohyeddin Assali

Abstract

Globally, according to the World Health Organization, cancer is the second leading cause of death worldwide. In order to manage cancer, many approaches have been used, such as surgery, radiation, chemotherapy, and gene therapy.

Medicine research has taken advantage of biotechnology-based therapy in the past several years, and one of the newest strategies in cancer therapy; is the utilization of small interference RNA (siRNA) to control gene expression. However, effective delivery of siRNA into cells is a challenge, particularly in vivo. Lipofectamine is currently used *in vitro* for this purpose, but unfortunately, the compound has demonstrated unacceptable toxicity *in vivo*. To deliver these types of molecules without causing significant harm, researchers are developing new technological delivery systems. The development of drug delivery systems based on carbon nanotubes (CNTs) has received a lot of attention in this respect.

Our project aims to develop a new method for delivering siRNA into colon cancer cells in order to target the expression of the β-catenin protein, which is known to play a role in a variety of developmental processes; such as cell growth and proliferation, embryonic patterning, cell differentiation, and other cellular functions. The new approach is based on the synthesis of a new nano-system of multi-walled carbon nanotubes (MWCNTs) functionalized with a tetra-amine linker and mannose sugar as a targeting agent to increase the nano-system`s uptake and selectivity.

We successfully functionalized MWCNTs with tetra-amine groups (*f*-MWCNTs (8)), which were then functionalized with mannose molecules (*f*-MWCNTs (12)), confirmed by atomic force microscopy. In addition, the amount of amine in *f*-MWCNTs (8) was 12.7 x 10^3 nmol/mg and 40 x 10^3 nmol/mg in *f*-MWCNTs (12), while the amount of

loaded mannose in *f*-MWCNTs (12) was 20.02 μg/mg as confirmed by the anthrone method. The N/P ratio required to trap β-catenin siRNA starts at 5:1 for *f* -MWCNTs (8) and 15:1 for *f* -MWCNTs (12), as determined by agarose gel. Western blot analysis revealed that our compounds significantly reduced β-catenin protein expression ($p > 0.05$). The knockdown percentage was 20% in *f*-MWCNTs (8) and 50% of *f*-MWCNTs (12). We hypothesized that the possible up-regulation of mannose receptors on the surface of caco-2 cells may increase the transfection efficacy of *f*-MWCNTs (12) compared with *f*-MWCNTs (8).

The MTS results showed that the down-regulation of β-catenin protein can restrict cancer cell growth and prevent cell proliferation which was shown significantly in both transfection approaches with an IC50 equal to 66.48 for *f*-MWCNTs (8)-siRNA slightly lower than control (IC50 = 70.01μg/ml) while 19.32 μg/ml for *f*-MWCNT (12)-siRNA. Also, this effect can increase the efficacy of 5-FU in colon cancer significantly compared with control. Therefore, we propose that our approach could be implemented in the setting of colon cancer therapy.

Keyword: Beta-catenin; Colorectal Cancer; Multi-walled Carbon Nanotubes.

Chapter One
Introduction

1.1 Cancer

In 1976, neoplasms were first identified [1]. According to the World Health Organization, cancer can be defined as a large group of diseases that can develop in any cell or tissue when the cells skip the checkpoints in the cell cycle, avoid tumor suppressor signaling, inhibit apoptosis processes by activation of antiapoptotic Bcl2 genes, or inhibit the expression of genes that trigger cell apoptosis and start the uncontrolled division. Globally, cancer can be considered the second leading cause of death after cardiovascular diseases due to early diagnosis and lack of symptoms, accounting for an estimated 9.6 million deaths in 2018 [2].

It is still unknown what causes cancer, despite scientists' efforts, but cancer can be caused by several factors. Infectious agents, smoking, occupation, diet, environment, and genetics are all examples of cancer risk factors [3]. Many biological factors are required for cancer establishment and spread, such as cell death resistance (apoptosis), the ability to invade surrounding tissue and colonize distant locations to form regions with metastatic lesions, which is considered the major cause of cancer death. Cancer cells, like any type of cell, need nutrients to stay alive and to keep growing. These requirements are achieved by a process called angiogenesis, which means a physiological process through which new blood vessels are formed from pre-existing blood vessels by the secretion of high amounts of pro-angiogenic factors to form abnormal blood vessels characterized by disorganized, permeable, and immature blood vessels. The formation of these blood vessels formed a critical step in cancer growth, development, and metastasis by supplying oxygen, and nutrients as well as the removal of waste products [4, 5].

Cancer cells undergo a multistage process characterized by fast cell proliferation of abnormal cells and spreading to different body parts. When this occurs, experts say cancer has metastasized [6], Figure 1.A.

Figure 1.A

angiogenesis and metastatic process for cancer cells

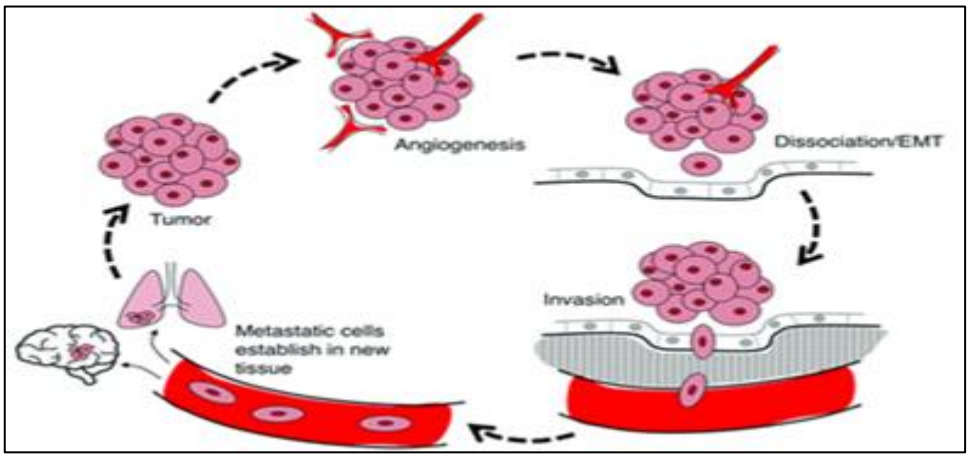

De Ieso, M.L. and A.J. Yool, *Mechanisms of aquaporin-facilitated cancer invasion and metastasis.* Frontiers in chemistry, 2018. **6**: p. 135.

Cancer presents a big challenge for experts. Despite its prevalence and deadly nature, colorectal cancer remains among the most common and deadly types of cancer. The problem persists despite the widespread use of preventive screenings as well as major advancements in treatment options. It is clear that cytotoxic and targeted therapies still have a long way to go in managing incurable metastatic disease and that tumors will eventually accumulate means to evade treatment, which ultimately leads to death [7].

Scientists employed a variety of interventional cancer prevention and treatment techniques, including surgery, radiation, chemotherapy, immunotherapy, and other approaches that utilize nonselective agents, resulting in several adverse reactions such as fatigue, loss of appetite, nausea, bowel issues, hair loss, and an increased risk of infections or the development of other types of malignancy [8-10].

In this regard, new approaches have been developed for cancer therapy, such as gene therapy or what some call nucleic acid therapy (NAT), which is considered an important and interesting approach. The strategy of gene therapy stands on using small molecules such as DNAs or RNAs and, in addition, utilizing the overexpressed proteins that result from several mutations in the genes of cancer cells. For instance, small RNAs have been investigated to suppress the expression of oncogenes by; targeting DNA repair, controlling cell growth and proliferation, etc. [11].

1.2 Small regulatory RNA (sRNA)

Noncoding RNA molecules called small regulatory RNAs (sRNAs) have a significant role in many cellular effects, such as the inhibition or activation of many processes. sRNA has a complex structure composed of several loops that contribute to sRNA`s binding to its targets. Living cells have a lot of types of sRNA. For example, antisense RNA, outer membrane protein regulation, housekeeping genes, and the regulation of RPoS. Antisense RNAs are single-stranded RNAs that can to complementary mRNA, resulting in inhibition of mRNA transcription.

There are two types of antisense RNA, which are cis and trans antisense genes. Cis antisense genes are encoded by the overlapping of antisense RNAs and their targets genes, while in the case of trans antisense genes, the antisense genes are separated from their targets genes which means there is no overlapping between them. Housekeeping genes such as tRNA, rRNA, snRNA, and snoRNA are unique types of genes that have a function in the regulation and maintenance of several basic cellular processes and homeostasis. Also, small RNAs can control RPoS gene translation. RPoS genes encode sigma factors, which regulate other types of transcription and stress. Furthermore, small regulatory RNAs also have a role in the regulation of many types of proteins in the cell membranes that are involved in controlling substances' entry and exit from the cell [12-14].

Many small RNAs (sRNAs), such as microRNAs (miRNA) and short interfering RNAs (siRNA) have been identified. Small interfering RNAs have a size ranging from 20 to24 nucleotides. Also, their exact functions have not been known or investigated. siRNAs are double-stranded RNA that comes from different sources, such as transposable elements (TEs), also known as jumping genes, natural sense-antisense pairs, tandem repeats, duplexes involving pseudogene-derived antisense transcripts, hairpin RNAs, convergent mRNA transcripts, and tandem repeats. RNA viruses and transgenes are also considered other sources of siRNA.

Furthermore, siRNAs have many types. For instance, heterochromatic siRNA (hc-siRNA), natural antisense transcript siRNA (nat-siRNA), trans-acting siRNA (ta-siRNA), and secondary siRNA. In addition, many siRNAs duplexes can be produced from one siRNA [13]. The mechanism of the siRNA that is showcased in Figure 1.2 B

arises from its distinctive structure of specific codons that selectively bind to the B-catenin mRNA, whose siRNA sequence is 5' -TTCTCCGAACGTGTCACGT-3'.

The mechanism starts when the siRNA is attached to two different subunits inside the cells which are Slicer and Aragonite to form a complex known as RISC. Then the RISC complex allows siRNA to bind to the complementary target mRNA causing silencing to the mRNA and preventing its translation [15], figure 1.B.

Figure 1.B

Non coading RNAs classification and siRNA mechanism of action

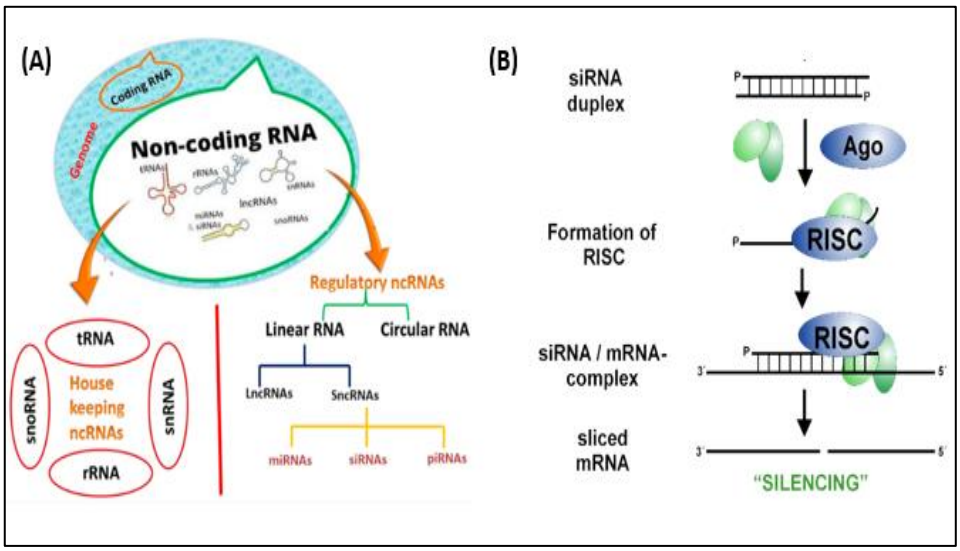

Almatroudi, A., Non-Coding RNAs in Tuberculosis Epidemiology: Platforms and Approaches for Investigating the Genome’s Dark Matter. International Journal of Molecular Sciences, 2022. **23**(8): p. 4430.

1.3 Beta Catenin

Beta-catenin (β-catenin) is a protein that is encoded by the CTNNB1 genes and is involved in cell adhesion and gene expression. Beta catenin is a subunit of calcium-dependent molecules (CAM), which is known as the cadren protein complex that acts as signal transduction for Wnt signaling pathways.

The Wnt signaling pathways are a set of signaltransduction pathways that use both autocrine and paracrine signaling. there are three types of Wnt signaling pathways that have been discovered which are the canonical Wnt pathway, the noncanonical Wnt/calcium pathway, and the noncanonical planar cell polarity pathway.

All three pathways are started via binding of the Wnt signaling pathway to its G-protein coupled receptor [12]. The first discovery of these signaling pathways was through their roles as proto-oncogenes for several types of cancer. For example, breast cancer, colorectal cancer, melanoma, prostate cancer, etc. Each of these types of signaling pathways has unique functions. The canonical Wan pathway activation, for example, is involved in the development of malignant and benign tumors. The noncanonical planar cell polarity pathway affects the cell shape by its action on the exoskeleton. Noncanonical Wnt/calcium pathway involved in Ca2+ regulation inside the cells.

There are several factors involved in overexpression of the beta-catenin complex, such asmutations in genes that are involved in its production, overexpression of wnt signaling pathways ligands, dysfunction of the wan pathway regulatory mechanisms, and over-production of PGE2 [16]. Several developmental processes, including cell growth and proliferation, embryonic patterning, and cell differentiation, are influenced by the Wnt family of transcription factors, which is a key regulator of stem cell biology [17].

High-glycosylated Wnt proteins are secreted ligands that bind with frizzled G-protein coupled receptors and low-density lipoprotein receptor-related protein 5/6 (LRP5/6) to activate cytoplasmic pathways [18].

As a key component of Wnt signaling, beta-catenin associates with Axin, Dishevelled (Dvl), glycogen synthase kinase 3 (GSK3), casein kinase 1 (CK1), and Adenomatous polyposis coli (APC) to form a disassembly complex that facilitates B-catenin phosphorylation by CK1 and GSK3 and subsequent breakdown of the protein. When the destruction complex separates in response to a Wnt-mediated signal, it permit B-catenin to enter the nucleus and interact with transcriptional regulators of the lymphoid enhancer-binding factor (LEF)/T cell factor (TCF) family, leading to the downstream transcription of genes that are involved in reducing cellular adhesion, boosting cell migration, and improving cell differentiation [19-21].

In addition, eta-catenin also plays a crucial role in the regulation of adherence junctions such as connecting N-cadherin to -catenin and the actin cytoskeleton [22]. The cellular response to Wnt largely depends on cell-intrinsic characteristics that may change over time during development [23], figure 1.C.

Figure 1.C

Types of wnt pathway

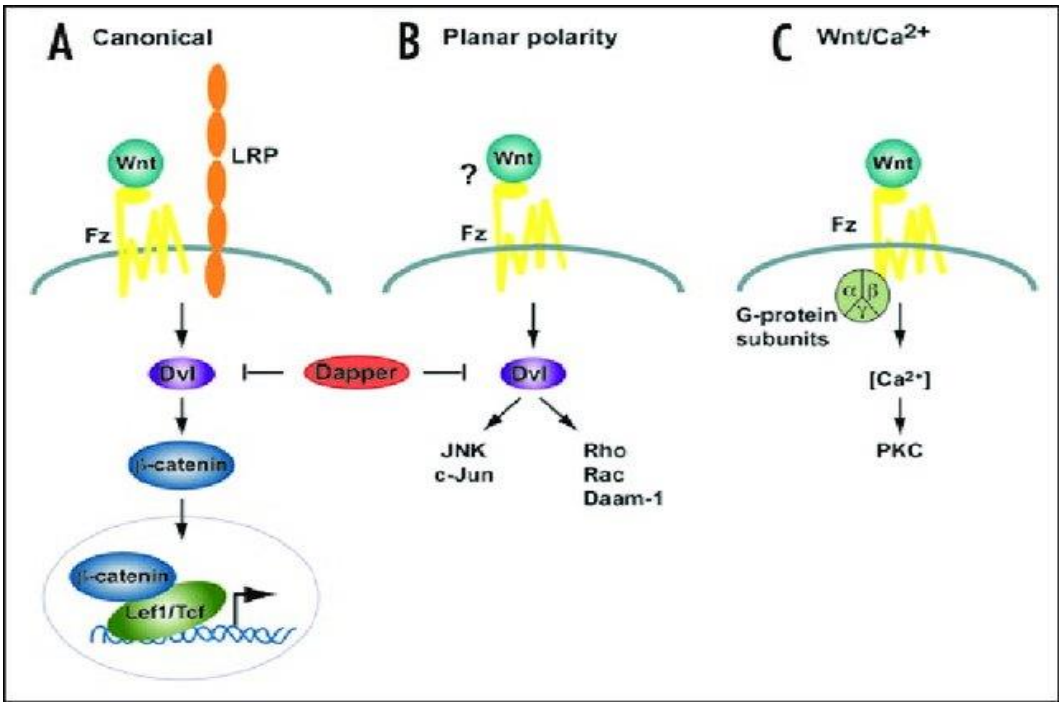

Boras-Granic, K. and J.J. Wysolmerski, Wnt signaling in breast organogenesis. Organogenesis, 2008. **4**(2): p. 116-22.

1.4 Gene Delivery

Gene delivery technology is a system that is used to deliver a specific gene safely and effectively. Induction of effective gene expression depends on the route of the drug to be administered, the targeting system, and the type of delivery system. Viral vectors are a gene delivery system based on viral particles that are no longer pathogenic by mutating genes that respond to their pathogenicity. Compering to non-viral victor, using of viral as delivery system has several concerns such as cell toxicity, immunogenicity and inflammation [24].

The life cycle of the viral vector starts with membrane attachment and internalization by endocytosis without affecting the endosome followed by the release of the plasmid either in the cytoplasm or the whole complex being entered into the nucleus and then getting released to begin gene expression. Adenovirus, Adeno-associated virus, Retrovirus, Herpes simplex virus (HSV), Epstein-Barr irus (EBV), and Lentivirus are examples of viruses that are used in gene delivery [25-28].

Non-viral vectors have superiority in gene delivery compared to viral delivery in that; are considered safer and lack antigenicity. The gene in this method is delivered to the cells after a physical opening in the cell membrane via physical or; electrical methods, and several kinds of nanomaterials are designed to serve these approaches, for example, liposomes, graphene, biodegradable polymeric NPs (PNPs), quantum dots (QDs), carbon nanotubes (CNTs), etc. [29-32], figure 1.D.

Figure 1.D

Cancer gene therapy approach

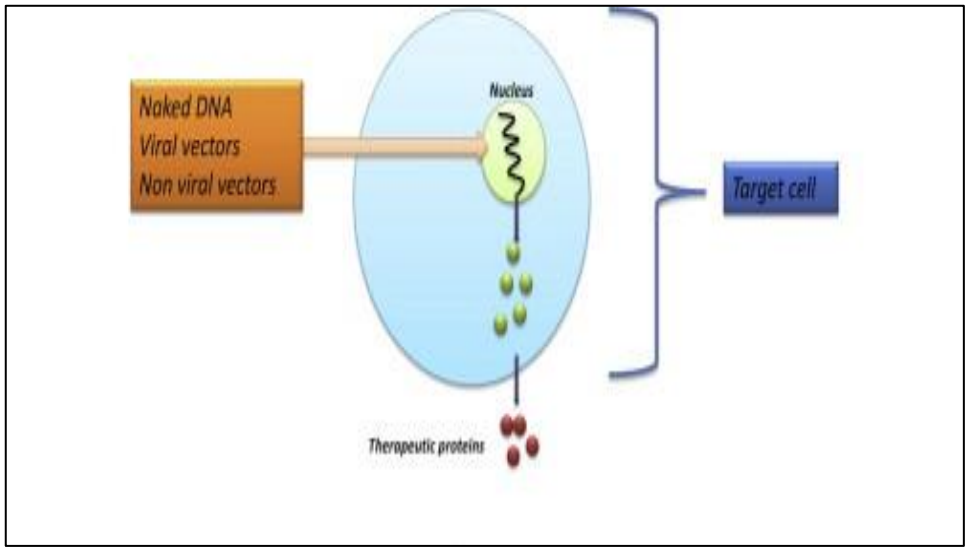

Singh, V., N. Khan, and G.R. Jayandharan, Vector engineering, strategies and targets in cancer gene therapy. Cancer Gene Therapy, 2022. **29**(5): p. 402-417.

1.5 Lipofectamine

A cationic liposome is a spherical structure containing positively charged lipids. The size of cationic liposomes can range from 40 nm to 500 nm, depending on whether one or multiple layers are present; they are then classified as bilayer liposomes or multilayer liposomes [33].

Through ionic interactions with negatively charged phosphate groups of the nucleic acids (DNA, mRNA, and siRNA), cationic liposomes form complexes with positively charged phospholipids. Clusters of aggregated vesicles form when cationic liposomes interact with nucleic acids [34].

Due to these interactions, after condensing the cationic liposomes, they will be able to encapsulate several therapeutic and diagnostic agents within their aqueous compartment as well as within their lipid bilayer due to that interactions. [35, 36]. Liposomal liposome-based Lipofectamine 2000 is a cationic liposome-based transfection reagent used for in vitro transfection of a variety of mammalian cells with high transfection efficiency. There are several experimental variables that determine transfection efficiency and cell viability, including liposome and DNA concentrations, cell density, liposome-DNA complexing time, and the presence of serum and antibiotics [37]**.**

Lipofectamine reagent was widely used for transfection, but now there is concern about its toxicity. The toxicity of Lipofectamine 2000 may adversely affect its use in most cells, which compromises its transfection efficiency [38]. The toxicity of lipofectamine arises from its positive charge, which can interact and form complexes with plasma proteins in the blood; and stimulate the immune system through the opsonization mechanism [39]. Adding polyethylene glycol (PEG) derivatives to the surface of cationic liposomes can reduce this cytotoxic effect [40], figure 1.E.

Figure 1.E

Transfection mechanism of the Lipofectamine

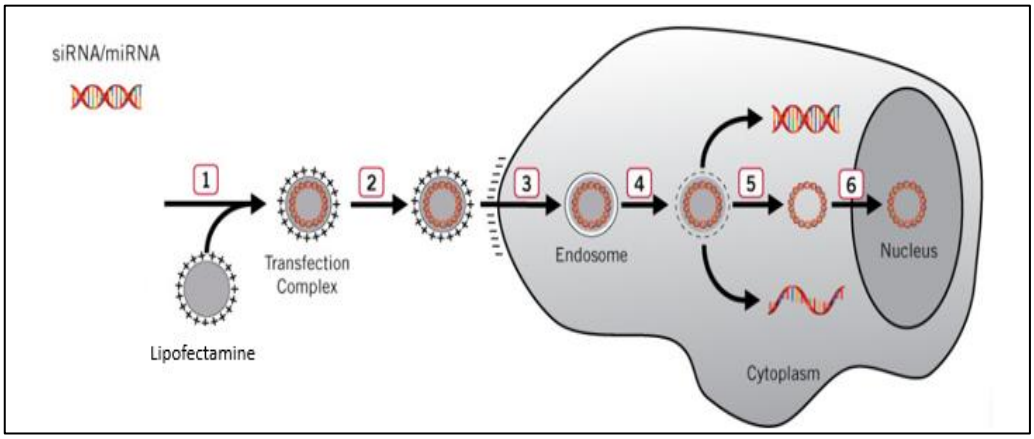

LLC, M.B. What is Transfection? 2022 [cited 2022 8/8]; Available from: https://www.mirusbio.com/transfection.

1.6 Carbon Nanotubes

An application of anotechnology in medicine is called “nanomedicine,” which is based on three powerful molecular technologies, first of all, there are nanoscale-structured materials and devices, which are used especially in smart drugs, targeted drug delivery, and advanced diagnostic biosensors [41].

Secondly, use it in artificially engineered microorganisms, genomics, and proteomics. Finally, use it in a machine like a nanorobot used for diagnosis, delivery, and even destruction of the cause of the disease [42]. A lot of nanomaterials are used in this field, and one of the most important nanomaterials is called carbon nanotubes [41-44], figure 1.F.

Figure 1.F

The graph illustrates where nanoparticles lie in the nanoscale

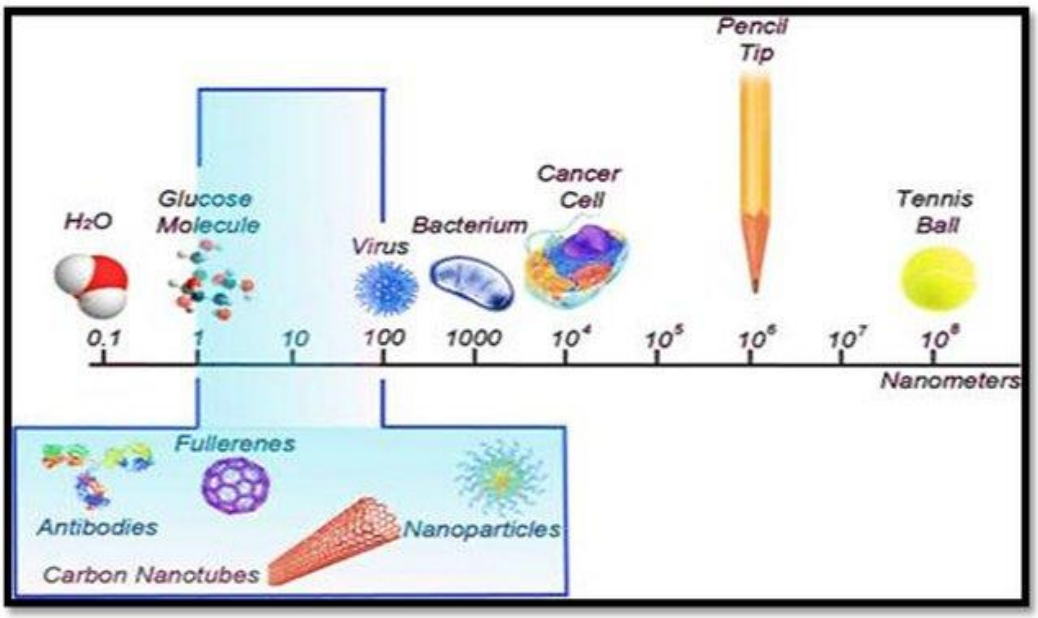

El-Diasty, A.I. and A.M. Ragab. Applications of nanotechnology in the oil & gas industry: Latest trends worldwide & future challenges in Egypt. in North Africa Technical Conference and Exhibition. 2013. OnePetro.

The discovery of carbon nanotubes (CNTs) was made by Sumio Iijima in 1991 [18]. Carbon nanotubes can be described as hollow cylindrical sheets mainly made up of carbon as like as graphite, they have long about 2 mm and carrying capacity higher than cooper around 1000X, thermal stability can reach around 4000 k, light in weight, also they have needle-like structure so they can penetrate the cell membrane of cells in ease

and due to the large surface area of the carbon nanotubes and a lot of molecular material can be loaded on its surface [45-52].

According to the natural design of carbon atoms by which it is made up, they can be classified into single-walled CNTs, polymerized single-walled CNTs, multi-walled CNTs, nano buds, nano homes, etc. Most experiments focused on single-walled carbon nanotubes (SWCNTs) and multi-walled carbon nanotubes (MWCNTs). SWCNTs are long-warp graphene, hile MWCNTs are made up of many SWCNTs stacked on top of each other, figure 1.G [53].

Figure 1.G

Structure of SWCNTs and MWCNTs

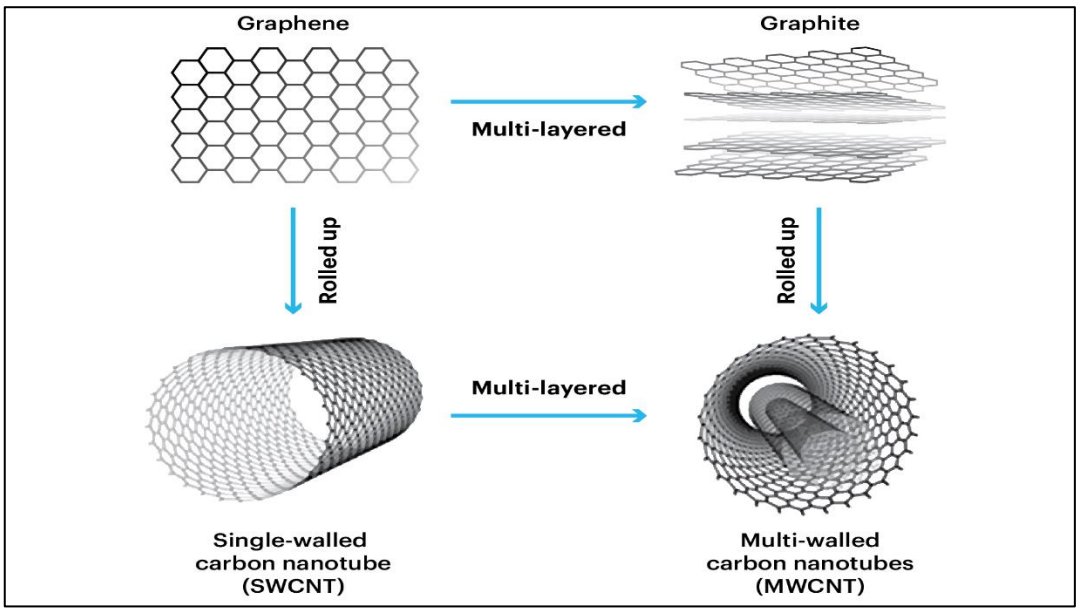

Marina Filchakova, V.S. Single-walled carbon nanotubes: structure, properties, applications, and health & safety. 2022 [cited 2022 8/8]; Available from: https://tuball.com/articles/single-walled-carbon-nanotubes.

Studies show that three main approaches are being used to synthesize CNTs. For instance, using the chemical vapor deposition (CVD) technique, a melted and decomposed hydrocarbon such as acetylene is implanted in holesin a silicon sheet alongside iron nanoparticles at the bottom of it to take the shape of the tunnel. There are many types of CVD, such as catalytic chemical vapor deposition (CCVD), which is the most common, microwave plasma (MPECVD), radiofrequency CVD (RF-CVD), and hot-filament (HFCVD) [54].

The laser ablation (LA) technique mainly depends on the physical properties of metals and the environmental medium. A laser beam is directed at the metal, resulting in photoionization of the plate, which is followed by the release of metallic nanoparticles from the targeted metallic plate [55]. Arc Discharge Method (AD), which involves the use of two graphite electrodes. Anodes could be either pure graphite or mixed with metals. An arc is struck between the electrodes in a controlled atmosphere (low pressure). The distance between the electrodes is reduced until a current of 50-150 A is present, at which point the temperature in the anode rises to the point where carbon sublimes and a plasma forms [55].

Carbon nanotubes have several applications in science, medicine, and biology in both therapeutic and diagnostic applications due to their special chemical, physical, thermal, and electrical properties [56]. In medical neurology, they are applied as a scaffold for neurons and stem cells to facilitate their growth and differentiation; they are also applied for neuronal electrical stimulation and detection [57]. In physics, as another example, carbon nanotubes are used to give an accurate measurement for the dose deposit of beta particles from a strontium 90 source [58-61].

Carbon nanotubes can be distributed in the cell cytoplasm after penetration of the cell membrane, at which point they will affect the physiological functions of the cells, and this effect is dose-dependent. This effect increases and becomes more harmful, especially with CNTs associated with metal [62-64].

Carbon nanotube toxicity depends on different factors that cause toxicity through different mechanisms, for example, hydrophobic character, low water solubility, exposure duration, and concentration, method of preparation, and purification, diameter length, types of functionalization, amounts of loaded amounts and method of exposure. [65]. The reproductive and developmental systems, the cardiovascular system, and the pulmonary system are the common body systems that are affected by CNT toxicity. Due to previous problems associated with CNTs, they have limited their application in the biomedical field. Moreover, many studies showed that the toxicity of carbon nanotubes varied between dispersed and non-dispersed CNTs, thus, it is necessary to produce carbon nanotubes with modified surface characterizationby functionalization [66, 67].

CNT toxicity has been evaluated in vivo in several studies. In animal studies, inhaling CNTs caused lung damage, especially when they had large diameters. Additionally, CNTs are genotoxic to the lungs without harming the hematopoietic system such as bone marrow, spleen, liver, kidney, and others if inhaled directly or instilled intratracheally. By using short lengths and diameters of CNTs, CNTs' toxicity can be reduced.

This can be done by functionalizing CNTs with a massive amount of biocompatible materials such as tetra-amine with tetra-ethylene glycol, mannose, and surfactants for instance TWEEN. Furthermore, using that strategy will increase CNT's dispersibility and biocompatibility as well as decrease their accumulation and increase elimination from the body through feces and renal [68-70].

1.7 Functionalization of CNTs

Due to the high surface energy and hydrophobic character of CNTs, they are intended to be agglomerated in aqueous media. This agglomeration limits their application in the medical field. To solve these problems, scientists used different strategies to improve CNTs' dispersion in aqueous media, namely chemical and mechanical strategies. A physical strategy is done by using high shear and impact mixing, ultra-sonication, and rubbing [71].

This method separates the carbon nanotubes but on the other hand, it can also destroy them, so this approach is considered an effective approach. While the chemical approach aimed to alter the chemical surface of CNTs by either covalent or noncovalent functionalization, functionalized CNTs have chemical, physical, electrical, and optical properties different from the non-functionalized (original) carbon nanotube [72, 73], figure 1.H.

Figure 1.H

Covalent and non-covalent functionalization of CNTs

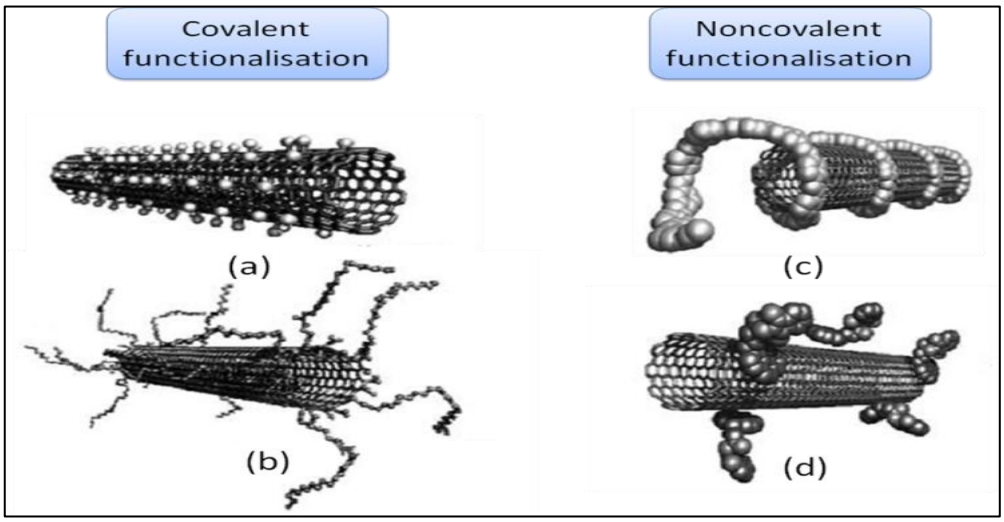

Beyou, E., et al., Polymer nanocomposites containing functionalised multiwalled carbon nanoTubes: a particular attention to polyolefin based materials. Syntheses and applications of carbon nanotubes and their composites, 2013. **1**: p. 77-115.

1.7.1 Noncovalent functionalization of CNTs

The interaction of Van der Waals forces between the molecules and carbon nanotubes causes this type of functionalization. For instance, surfactants, polymers, and aromatic chemicals can be employed to modify the surface of nanotubes [74-76].

The CNTs' electrical characteristics are maintained by the non-covalent functionalization, but they remain sensitive to pH, salt concentration, and other conditions. As a result, the deposited moieties on the surface of carbon nanotubes do not release before the CNTs reach their target site [77]. In this regard, Assali and his team developed a technique for improving the bio-performance of nanomaterials, by incorporating neoglycolipids into the surfaces of CNT compounds via non-covalent interactions known as π–π stacking.

To achieve improved hydrophilic-hydrophobic balance, they created the neo-glycoconjugate structure, which consists of a pyrene tail attached to the glycol ligand (sugar head) as a spacer. Similar to glycol conjugates, these aggregates can cause various ligand-lectin interactions somewhere at the cell membrane [78], figure 1.I.

Figure 1.I

Noncovalent functionalization of CNTs

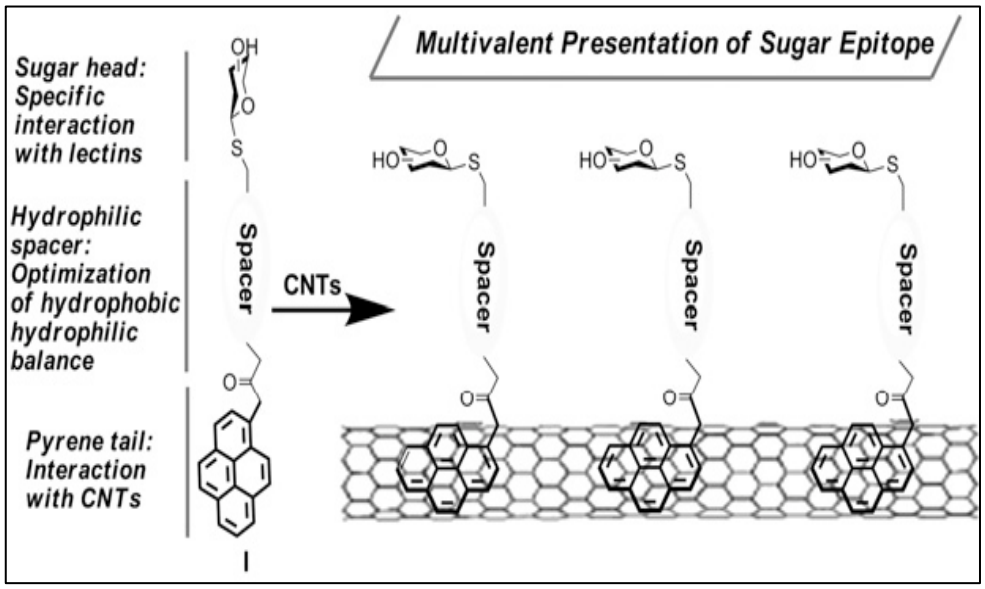

Assali, M., et al., Non-covalent functionalization of carbon nanotubes with glycolipids: glyconanomaterials with specific lectin-affinity. Soft Matter, 2009. **5**(5): p. 948-950.

1.7.2 Covalent functionalization

It is possible to achieve covalent chemical modification by oxidation reactions [78], arylation, additional reactions, and other reactions involving other reactive species [79]. The electrical characteristics of CNTs are altered by covalent functionalization, which shifts the hybridization of carbon from sp2 to sp3. As a result of this functionalization, an associated biomolecule cannot be released before it reaches the target site, thereby minimizing its negative effects [80-82], figure 1.K.

Figure 1.K

Covalent functionalization of CNTs

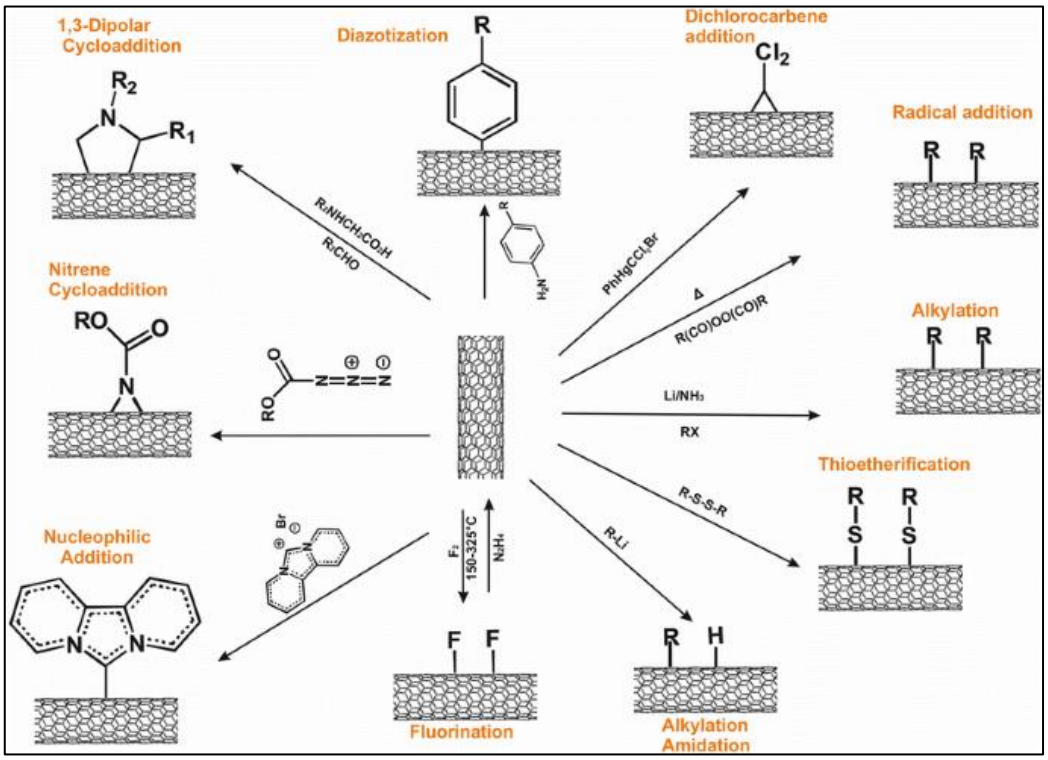

Syrgiannis, Z., M. Melchionna, and M. Prato, Covalent carbon nanotube functionalization. 2015.

1.7.3 Fluorouracil (5-FU)

5-Fluorouracil (5-FU) is the prototype drug of the Fluoropyrimidines anti-cancer drugs. 5-FU is a pyrimidine analog and has a fluorine atom in the uracil ring at position 5. The anti-cancer activity of this drug comes from preventing the conversion of deoxyuridylic acid (dUMP) to thymidylic acid (dTMP) by inhibition of thymidylate synthase. Due to this, cancer cells are deprived of thymidine in the S phase of the cellular replication cycle, which is essential for cell growth and DNA synthesis [83].

Also, 5-FU undergoes metabolism by further alternative enzymes, which can lead to the production of several metabolites that are incorporated into the DNA, consequently distorting protein production [84]. 5-Fluorouracil (5-FU) is an essential component of systemic chemotherapy for colorectal cancer (CRC) in the palliative and adjuvant settings [85], figure 1.L.

Figure 1.L

5-FU structrer and mode of action

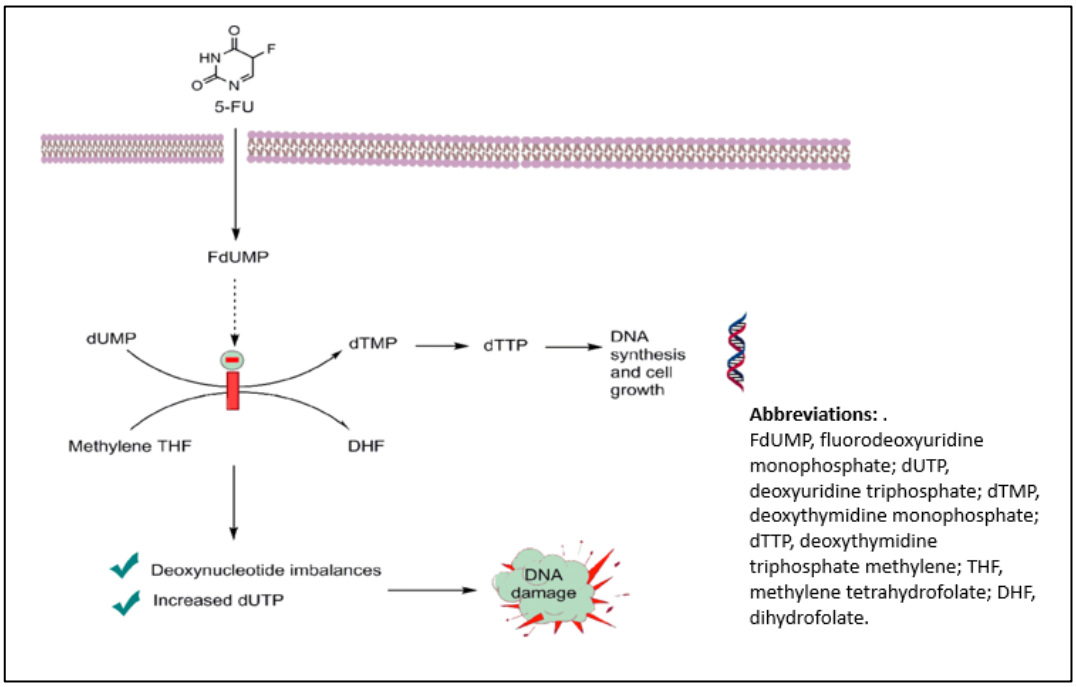

Entezar-Almahdi, E., et al., Recent advances in designing 5-fluorouracil delivery systems: a stepping stone in the safe treatment of colorectal cancer. International journal of nanomedicine, 2020. **15**: p. 5445.

Through its role in inhibiting proliferation or inducing programmed cell death, p53 plays a crucial role in the cellular stress response. As well as determining the cellular sensitivity to 5-FU, p53 plays a major role in the anti-cancer effect of 5-FU [84, 86, 87]. Regarding the molecular mechanism of 5-FU, the drug has the ability to increase the translation, stability, and intensity of P53 activity. Also, the P53 target gene is able to stimulate several tumor suppression processes such as apoptosis, cell cycle arrest, and the sensitivity of colorectal cancer to 5-FU [88]**.** A growing body of information indicates that p53 plays additional roles in a variety of biological processes when it cooperates with other signaling pathways.

Several studies show that p53 has a role in regulating the death of cancer cells as well as their survival via activation of the Wnt pathway, which means that while the drug kills cells by activatingP53, it also promotes their growth [89, 90]. Cancer stem cells (CSCs) play an important role in the clinical benefits of chemotherapies [91]. These cells undergo an endless cycle of self-renewal and differentiation, resulting in the formation of tumor-initiating cells. As a consequence, CSCs allow chemotherapy-treated tumors to

relapse [92]. CSC markers have been reported to be associated with poor overall survival after chemotherapy in advanced CRC patients [93, 94]. Furthermore, emerging evidence suggests CSC eradication can contribute to overcoming chemotherapy failure by preventing tumor recurrences through the eradication of CSCs enriched by 5-FU-based therapies [95-97]. Yong-Hee Cho and a co-worker demonstrate that activation of CSCs by 5-FU can induce the transcription factor of the WNT/β-catenin pathway in the colorectal cancer cell line, so combination therapy between 5-FU and Wnt inhibitors can prevent cancer cell growth and prevent disease relapse and recurrence [98].

1.8 Literature Review

In June 2008, Mai YJ and co-workers investigated the use of specific siRNA to inhibit beta-catenin expression and examined its effects in two types of cells, which are Jurkat and K562 cells. In that trial, scientists used specific siRNA to knock down beta-catenin expression, and scrambled siRNA was used in the control group. For quantification of mRNA and protein amounts of beta-catenin, they used Real-time polymerase chain reaction (PCR) and Western blot, respectively. In addition to that, viable cells were counted using the refusal-dyed trypan blue method to determine the growth curve. Also, MTT and clonogenic counting were used to determine cell proliferation, Annexin V/PI staining was used to measure the percentage of apoptotic cells, and based on propidium iodide staining, a cell cycle analysis was performed. The results showed that the beta-catenin-siRNA transfected group exhibited a significantly lower survival, clonogenicity, and proliferation rate than a control group transfected with scramble siRNA [99].

Another study conducted by Li K et al. investigated the effect of short interference RNA (siRNA) on the Wnt/-catenin signaling pathway activity as well as the proliferative, apoptotic, and invading capacities of the human colon cancer cell line SW480. In order to achieve this, double-stranded siRNA (beta-catenin-siRNA) was created and transfected into SW480 cells. For mRNA and beta-catenin to be detected, PCR and western blotting were applied respectively. The 3-(4,5-dimethylthiazol-2-yl)-2,5-diphenyltetrazolium bromide assay was used for a treasure trove of cell proliferative capacity, while flow cytometry and a caspase-3 activity assay, respectively, were used to identify cell apoptosis. To examine the impact of siRNA-mediated gene silencing on the invasion and metastasis of SW480 cells in vitro, a matrigel invasion experiment was carried out. The results showed that mRNA and beta-catenin protein expression was

decreased in transfected cells with siRNA compared with negative control, liposome group, and negative control as well as proliferation, apoptosis, and invasion decline [100].

In April 2010, Teng Y et al, conducted an experiment to investigate the effect of down-regulation of beta-catenin on the Wnt/beta-catenin pathway in lung adenocarcinoma A549 cells through specific siRNA that was transfected to calls via plasmid. During the trial, the cancer cells were grouped into three categories. The first one was the transfected group with siRNA via a plasmid called PGCsil-CTNNB1-siRNA, a negative control group (plasmid without siRNA), and a blank (non-transfected group). Among each group, beta-catenin and cyclin D1 were detected using real-time PCR (Wnt/beta-catenin pathway targeting genes). To study the proliferation capacity of the cells, an MTT proliferation assay was performed. Analyses of the cell cycle were carried out using flow cytometry. To evaluate cells' clone formation and migration capabilities, clone formation experiments and millicell chambers were performed. In PGCsil-CTNNB1-siRNA cells, beta-catenin and cyclin D1 mRNA expression decreased. Comparatively, it was lower than that of the negative control group and the blank control group. Additionally, compared with negative controls and blank controls, proliferating capacity was inhibited on Days 5-7, with cell-doubling times of 56.18 h being significantly longer than 37.9 h for the negative control group and 34.2 h for the blank control group, as well as an increase in the number of G0-G1 cells compared to the negative control (73.8%+/-0.9%, $P<0.01$) and blank control groups (75.8%+/-1.5%, $P<0.02$) was observed, and in the PGCsil-CTNNB1-siRNA group, the clone formation ratio was decreased. After the study's completion, the researcher came to the conclusion that knocking down beta-catenin reduces lung cancer A549 cells' ability to proliferate, form clones, and migrate in addition to inhibiting the Wnt/beta-catenin signal transduction system. As a result, it might become a new target for treating lung cancer [101].

Yu F and Associates conducted an experiment to examine the changes in laryngeal cancer Hep-2 cells to cisplatin following the inhibition of -catenin gene expression by siRNA. The experiment was divided into three parts, the first one was Hep-2 cells with siRNA, the second was a negative control, and the third was blank. After the Hep-2 cells were transfected with siRNA, the mRNA and protein levels were quantified by

using PCR and western blotting respectively. MTT test was conducted to assess the cell proliferation in different concentrations of cisplatin. Also, they determined the IC_{50} value, or inhibitory effective concentration, at 50%. After the cells were stimulated with identical doses of cisplatin, they measured the change in the apoptosis rate of three different groups of cells using flow cytometry. The results showed that siRNA significantly decreases beta-catenin expression, which causes an increase in cancer cells sensitivity to cisplatin [102]. Another investigation was conducted by Liyan W. and associates to ascertain the impact of siRNA-mediated beta-catenin silent gene expression on the cell cycle and apoptosis of various hepatoma cells. The siRNA transfection was done by using a bacterial plasmid. The results obtained showed that the mRNA level and beta-catenin expression were declining while apoptosis increased and the cells were blocked at the G0/G1 phase [103].

Also in October 2010, Wang XH and co-authors performed a trial to demonstrate the role of the Wnt/-catenin signaling pathway in the development of hepatocellular carcinoma (HCC). In order to achieve that, small interfering RNA (siRNA) targeting beta-catenin was created, produced, and transfected into HCC. The data showed that the levels of mRNA and beta-catenin decreased significantly. Furthermore, a substantial reduction in tumor cell prefiltration was observed. While molecularly, after 72 hours of beta-catenin siRNA transfection, Smad3, p-caspase-3, and Grp78 protein expression were all increased, whereas TERT, caspase-3, XIAP, MMP-2, MMP-9, VEGF-A, VEGF-c, and bFGF protein expression were decreased. However, following transfection, there was no difference in the expression of STAT3 and the HSP27 protein [104].

Recently, in April 2019, Zhang JG and co-workers aimed to inspect the effect of the knockdown of beta-catenin protein expression on multiple myeloma cells' drug resistance. The results showed that decreased expression of beta-catenin, as well as the Wnt/beta-catenin signaling pathway, caused a decrease in the IC_{50} of melphalan from (5.29±0.19) μmol/L to (1.88±0.64) μmol/L. Additionally, the percentage of cells that undergo apoptosis when exposed to melphalan increased from (35±0.5)% to (54±0.4)% [105].

In November 2020, Chen W et al, aimed to mitigate the peritoneal dissemination of resistance-type gastric cancer. A nanocarrier was created using aptamer-siRNA chimeras (Chim)/polyethyleneimine (PEI)/5-fluorouracil (5-FU)/carbon nanotubes (CNT)/collagen membrane, which was composed of 15 layers of 70-100 micrometers thickness.

Following the synthesis of nano-carriers, the results showed that the aptamer-siRNA chimera could target gastric cancer cells and silence drug-resistant genes by delivering 5-FU. Furthermore, in vitro experiments demonstrated that Chim/PEI/5-FU/CNT nanoparticles inhibited the invasion and proliferation of 5-FU-resistant gastric cancer cells. Preclinical trials on animals showed that the nano-system was able to significantly inhibit the sub-type of kinases called mitogen-activated protein kinase (MAPK) and was effective in treating gastric cancer with peritoneal dissemination resistant to 5-FU.

Furthermore, compared with the control group, which was composed of siRNA/PEI/5-FU/CNT, their nano-system was able to decrease the ki-67 proliferation index and expression of matrix metallopeptidase 9 (MMP9) significantly while showing a marked increase in the number of apoptotic cells. At the end of the study, the researchers concluded that an effective treatment for peritoneal dissemination of drug-resistant gastric cancer can be constructed using a chimera, PEI 5, 5-FU, CNT, and collagen membrane [106].

As a part of the immunotherapy of hepatocellular carcinoma (HCC). Niu Q and a coworker constructed a nanoparticle composed of Durvalumab, CNT, polyethyleneimine (PEI), and an aptamer-siRNA (chimera/Durmab/CNT) system. Experiments in vivo and in vitro demonstrated that specific binding of the nanosystem was observed for HCC cells and that it inhibited myeloid receptor-2 (Trem2) expression, whereas normal liver and lung did not show any effect on Trem2. As determined by chemical analysis, CNT/PEI nanoparticles have a diameter of 20-30 nm and a length of 200-350 nm, as shown by transmission electron microscope (TEM) analyses. On CNTs, there is evidence of dense PEI attachment.

Furthermore, Durvalumab might be released continuously for 48 hours under the control of CNT/PEI nanoparticles. Results from in vitro experiments showed that their nanoparticles could boost T lymphocytes and CD8+ T cell proportions and then induce HepG2 cell death. The pharmacological impact was also advantageous to those of the

aptamer/Durmab/CNT and Durmab/CNT positive controls. Additionally, the researchers revealed a tumor-bearingmouse model. The results showed that the nanocarrier greatly slowed the growth of the grafted tumor, further decreased its volume and expansion, and significantly boosted the death of HCC cells compared to controls [107].

In January 2010, Ye and colleagues targeted a signaling pathway that manipulates tumor growth to induce Caco-2 cells to enter the cell cycle from G0. The colon cancer Caco-2 cells were stimulated with epidermal growth factor (EGF). FACS analysis and (PCNA) staining were used to investigate the cell cycle and cell proliferation, and MTT assays were performed to assess the synergistic effects of EGF with chemotherapy. It was found that EGF significantly reduced the percentage of Caco-2 cells in the G0 and G1 phases by about 20%, while it significantly increased the cells' entrance into the S and G2/M phases. 5-Fluorouracil (5-FU) coupled with EGF improved the chemosensitivity of caco-2 cells to 5-FU, up to approximately three times greater sensitivity compared to 5-FU alone [108].

1.9 Aim of the project

The project aims to develop a new method for delivering siRNA in colorectal cancer cells that target β-catenin protein. The new approach is based on the synthesis of a new nanosystem of multi-walled carbon nanotubes (MWCNTs) functionalized with a tetra-amine linker and mannose sugar as targeting agents to increase the nanosystem`s uptake and selectivity.

1.10 Objectives

1. Functionalization of MWCNTs with a tetra-amine linker to form a complex with siRNA specific to beta-catenin protein and mannose sugar as targeting agents and then the characterization of the obtained compounds with the different analytical techniques.
2. Tests *f*-MWCNTs-siRNA complex formation by agarose gel electrophoresis and quantifies the amounts of β-catenin knockdown by the siRNA using western blot after transfection.
3. Determine the effect of knockdown β-catenin protein by siRNA on the cancer cell's proliferation and anti-cancer activity of 5-Fluorouracil.

1.11 General Methods for MWCNT Production and Functionalization

This thesis aims to mono-functionalize MWCNTs with tetramine linkers and bi-functionalize MWCNTs with tetramine linkers and mannose as a targeting agent. A click reaction was used to mono- and di-functionalize the MWCNTs-alkyne with the prepared tetramine linker, as shown in Scheme A.

Scheme A

Functionalization of MWCNTs with mannose sugar and tetra-amine linker

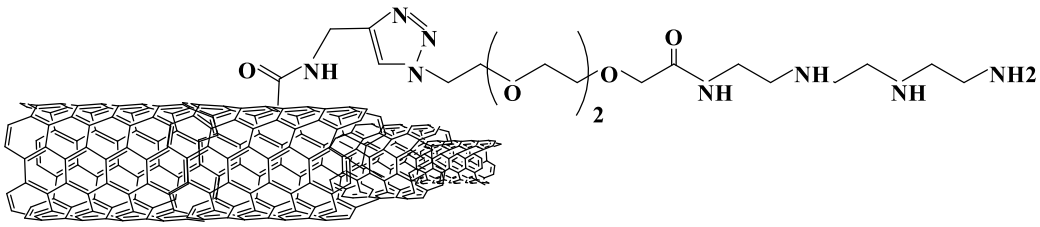

(8)

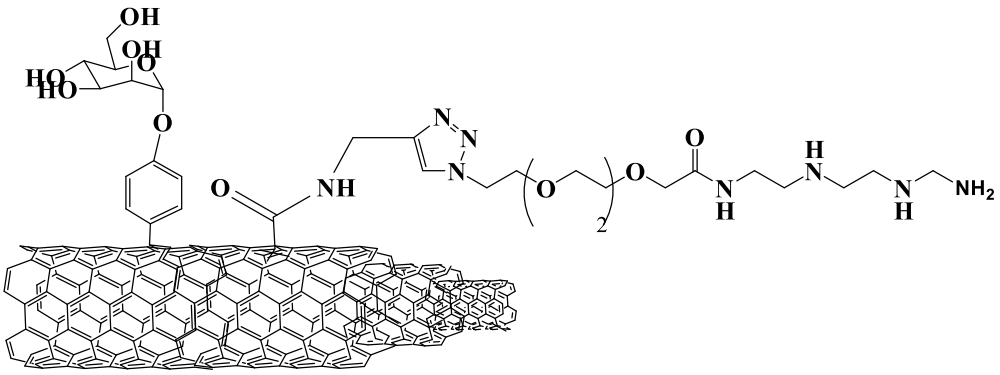

(12)

Chapter Two
Materials and Methods

2.1 Materials and Reagents

For the synthesis of our nano-system and chemical tests, we used the following materials and reagents: from Alfa Aesar company which is located in England, we purchased tetraethylene glycol (TEG) (catalog # B23990), 1-(3-Dimethylaminopropyl)-3-ethyl carbodiimide hydrochloride (EDC) (catalog #A10807), TBTU (catalog# B23597), propargylamine (catalog # H53495), trifluoroacetic acid (TFA) (catalog # A12198), and 4-nitrophenyl-α-D-mannopyranoside (catalog # N01C012).

From RiedeldeHaën Company in Germany, we purchased 1,2- Dichlorobenzene (o-DCB) (catalog # 65152) and Sodium azide (catalog # 0E30428). From Sigma-Aldrich company in the USA, we purchased iso-amyl nitrite (catalog # 110463), Mannose (catalog# SLBH1709V), palladium on carbon (catalog # 101375286), and toluene-4-sulfonyl chloride (catalog # 1234411), Silica gel, N, N-diisopropylethylamine (DIPEA) (catalog # 496219), di-tert-butyl dicarbonate (BOC2O) (catalog # 101281549), ethyl trifluoroacetate (catalog # A821163), 4-(dimethylamino) pyridine (DMAP) (catalog # 1122583). (ACROS OrganicsTM) provided us with 60% triethylenetetramine (catalog # 34407). isopropyl alcohol, disodium hydrogen phosphate, potassium dihydrogen phosphate, Anthrone, sodium hydroxide, sodium chloride, Acetone, dichloromethane (DCM), ethanol (EtOH), and methanol (MeOH) were purchased from C.S.

Company in Haifa. In addition to chloroform (Catalog # 67-66-3), diethyl ether (Catalog # 38132) and triethylamine (Catalog # 40502L05) were acquired from Merck Millipore and Carlo Erba Company, MI, in Italy provided the tetrahydrofuran (THF) solvent (catalog #487308). A purchase of N-Dimethylformamide (DMF) from Frutarom Laboratory Chemicals (catalog # 55145) was also made. In addition to chloroform (Catalog # 67-66-3), triethylamine (Catalog # 40502L05) and diethyl ether (Catalog # 38132) were acquired from Merck Millipore.

Also, from Frutarom Company localized in Haifa we purchased acetonitrile (CH3CN) (catalog # 5550070) solvents and n-hexane (Hex) (catalog # 2355544800024). For the nanomaterials that we used in our project, for instance carboxylated single-walled and

multiwalled carbon nanotubes, we purchased them from suppliers of nanostructured and amorphous materials, in the USA. A PTFE filter (37070) manufactured by Sartorius Stedim Biotech GmbH is located in Gottingen, Germany. TLC (DC-Fertigfolien Alugeram ® Sil G/Uv254) was purchased from Macherey Nagel company in Germany. Phosphomolybdic acid hydrate in aqueous solution (catalog #221866) was purchased from (BD company, USA).

In the biological part, we used Dulbecco's free Ca+2 -phosphate-saline buffer (REF # 02-023-1A), Pen-Strep Solution (catalog #030311B), and L-glutamine solution (REF # 03-020-1B) which was purchased from Biological Industries, Jerusalem. Trizma base (Lot number SLBF2864V) purchased from Sigma Life Science. The Ponceau S solution (patch number SLBN3529V) was purchased from Sigma-Aldrich. A catalog number 05669 of RPMI was purchased from Manassas VA, USA (Manassas VA, USA).

From Sigma-Aldrich in the USA, we purchased the following items; Agarose (catalog # A2790), Trypsin-EDTA solution 1X (catalog # 59417C), Triazole Reagent (catalog #T46108), fetal Bovine Serum (catalog # C8065), MOPS (catalog # M9381), and trypan blue solution (catalog # RNBD6249). β-catenin siRNA (lot # C2719). The MTS (catalog # G3581) was purchased from Promega (USA). Broad Range Markers: SC-2361 purchased from Santa Cruz Biotechnology, Inc.

Novel Juice was purchased from BIO-HELIX CO., LTD. Roti-ImmunoBlock, which was purchased from Roth Company; Western Blotting Lumino Reagent, ImmunoCruz™ which was purchased from Santa Cruz Biotechnology,. Monoclonal antibodies such as monoclonal anti-β-catenin (as a primary antibody), monoclonal anti-β-actin (as a primary antibody), and anti-mouse peroxidase antibody (as a secondary antibody), all of them from Sigma-Aldrich.

2.2 Instrumentation

The absorption analysis was carried out using 10mm quartz cuvettes and a 7315 Spectrophotometer by Jenway (UK). Sonicator and water bath (Elmasonic S 70 H, Elma®, Germany). Rotary Evaporator (MRC, ROVA-100, laboratory equipment manufacturer). Centrifuge (UNIVERSAL 320, Hettich Zentrifugen, Germany). Centrifuge-DCS-16-RVT (Prevac, Canada) was used for 4 °C. Esco CO_2 cell culture incubator was used to incubate the cell line. Also, an Accumax Variable micropipette

with normal and long narrow gel loading tips was used. TGA screening was performed on the TAQ50 instrument with a flow rate of 20 cc/min under nitrogen with a range of 20-1000 ºC. AFM images were taken on coreAFM in Nanosurf, Switzerland. Unilab microplate reader 6000 (for reading the viability test). Western blot equipment: Gel combs, gel cassette, electrode chamber (i.e Xcell Surelock and Omni PAGE TETRAD Mini-Prot), power supply CS-300V, rolling brush, washing dis, electrophoresis tank, blotting cassettes, sponges, nitrocellulose filter paper (1704085-BIORAD), membrane (#A29542891-Amersham™protran™, from GE Healthcare Life Science.

Eppendorf Thermo mixer dry, Shaker, PH/ORP meter (by HANNA), Benchtop UV Transilluminator, Photodoc-it™ imaging system, XB-30 Flak Ice maker M.R.C LTD. gel electrophoresis equipment: power cables, tank lid, casting dams, gel tray, electrodes, buffer tank, power supply CS (BIORAD). The softwares that were used in this project were Chemdraw for drawing the chemical structures of the compounds, GraphPad Prisim (version 9) for the statistics, and ImageJ for the desitometric analysis of the western blotting bands.

2.3 Synthesis and characterization

2.3.1 Synthesis of Tosyl-TEG-OH (1)

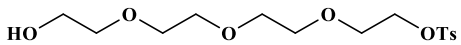

(1)

As a first step in synthesis,tetraethylene glycol 10 g (51.5 mmol)and 6 ml (51.5 mmol) of Et3N were added to 40 ml of THF. The mixture was stirred for 5 minutes, then 10 g (52.5 mmol) of tosyl chloride was added to the reaction gradually in an ice bath for 30 minutes. At room temperature, the reaction was then stirred overnight. On the next day, the obtained product was diluted with 200 ml of CHCl3, and it was washed using 50 ml of 1 molar HCl. After that, we added a drying agent, i.e., sodium sulfate. We used a rotovap to remove the excess solvent. CHCl3/MeOH (20:1) was used as the eluent for flash chromatography on silica gel to purify the remaining crude product. The yield of our pure compound was 37% (4 g, 14.4 mmol).

Retention factor (R_f): 0.51 of (9: 1) (Dichloromethane: Methanol).

^{1}H NMR (400 MHz, $CDCl_3$): δ 7.77 (d, 2H, J = 8.3 Hz, Ts), 7.33 (d, 2H, J = 8.0 Hz, Ts), 4.13 (t, 2H, J = 4.7 Hz, CH_2OTs), 3.66 (t, 2H, J = 4.9 Hz, CH_2CH_2OTs), 3.57-3.56 (m, 8H, $4CH_2O$), 3.50 (t, 2H, J = 5.2 Hz, CH_2CH_2OH), 3.27 (s, 2H, CH_2OH).

^{13}C NMR (100.6 MHz, $CDCl_3$): δ 144.8 (2CH Ar), 133.0 (2CH Ar), 129.8 (C Ar), 127.9 (C Ar), 70.7, 70.5, 70.2, 70.1 (CH_2CH_2OH), 69.2 (CH_2OTs), 68.6 (CH_2CH_2OTs), 40.3 (CH_2OH).

2.3.2 Synthesis of OH-TEG-N_3 (2)

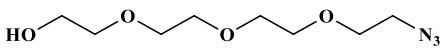

(2)

To synthesize product number 2, we dissolved 1.4 g (4.02 mmol) of compound 1 in 6 ml of EtOH thenadded 287.4 mg (4.42 mmol) of sodium azide. We stirred the reaction overnight at 70 ºCin reflux. On the next day, we removed the excess EtOH was removed by rotavap under vacuum. Then, the reaction was diluted with 100 ml of diethyl ether and washed with 50 ml of 1 molar HCl, after that, the organic layer was separated, and we added the sodium sulfate as a drying agent. The organic layer was then evaporated by rotavap, and we obtained a pale yellow oil material. The yield of our compound was 85% (1.23 g, 5.6 mmol).

R_f: 0.39 (DCM/MeOH 20:1)

^{1}H NMR (500 MHz, $CDCl_3$): δ 3.58 (t, 2H, J= 4.8 Hz, $HOCH_2CH_2$), 3.55-3.51 (m, 10H, 5 CH_2O), 3.46 (t, 2H, J = 4.8 Hz, $OCH_2CH_2N_3$), 3.26 (t, 2H, J = 4.8 Hz, $CH_2CH_2N_3$), 3.10 (bs, 1H, OH).

^{13}C NMR (125.7 MHz, $CDCl_3$): δ 72.5 ($HOCH_2CH_2O$), 70.6, 70.5, 70.4, 70.2, 69.9 (CH_2O), 61.5 (COH), 50.5 (CN_3).

2.3.3 Synthesis of COOH-TEG-N_3 (3)

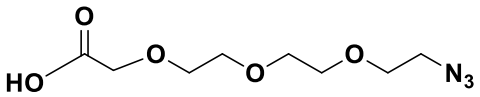

(3)

To synthesize compound number 3, we dissolved 450 mg (2.05 mmol) of compound 2 in 15 ml of both chronic acid and acetone. The reaction was stirred for 2-3 hours. After three hours, we added drops wise of isopropanol until the color became blue. Filtering the rxn with silica gel was performed. After that, we evaporate the remaining solvent by rotavap. In the end, we yielded 95% (342 mg, 1.45 mmol) of compound three.

R_f: 0.4 (DCM/MeOH 9:1).

^{1}H NMR (500 MHz, $CDCl_3$): δ 9.30 (bs, 1H, COOH), 4.15 (s, 2H, CH_2COOH), 3.80-3.60 (m, 10H, $5CH_2O$), 3.29 (t, 2H, J = 4.5 Hz, CH_2N_3).

^{13}C NMR (125.7 MHz, $CDCl_3$): δ 173.5 (CO), 70.9 (CH_2COOH), 70.4, 70.3, 70.2, 69.9, 68.3 ($OCH_2CH_2N_3$), 50.5 (CN_3).

IR: broad peak (2200-2600), 2921.63, 2853.17, 2108.78, 1714.41 cm-1.

2.3.4 Synthesis of Boc-protected tetraamine (4)

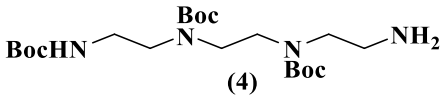

(4)

To synthesize Boc-protected tetraamine, we took several sequential steps. The first step is to add 70 ml of dry methanol to triethylenetetramine (745 µl, mmol) under the condition of vacuum-argon, then drops wise of Ethyltrifloroacetate (995 µl, 4.99 mmol) for 45 min was added under dry ice (-78 ºC).

After that, the reaction remained on the dry ice for a further 45 min. Then the reaction was put in ice (0 ºC) for one hour. After one hour, ten ml of dry methanol was mixed with 4.0 g (18.3 mmol) of Boc2O and added drop by drop to the stirred reaction. The reaction is stirred overnight. After 24 hours, we removed the methanol using a rotavapor device and diluted the remaining material with 60 ml of DCM.

Then, we extracted the reaction using a solution of 100 mg of NaHCO3 in 40 ml of DW. After that, we took the DCM layer (lower layer) and dried it with sodium sulfate. Then, we filtered the product, and DCM was evaporated to obtain a white powder. TLC was visualized by using (DCM: MeOH: NH4OH (10:1:0.1)), yielding 78%, (1.8 g, 8.2 mmol). After all of that, we dissolve the product in 70 ml of methanol and add to it a solution of 580 mg of K2CO3 in 5 ml of DW and then we refluxed the reaction at 70 ºC for 1 hour.

After six-hour, we evaporated the methanol and did an extraction by using 150 ml of DCM and 50 ml of DW. The organic layer was dried with sodium sulfate and then we filtered it and evaporated the DCM. The reaction was purified by using flash chromatography (DCM: MeOH: NH4OH (10:1:0.1)) to provide our interesting product, which is a triethylenetetramine-Boc compound. yield (44 %) (1.0 g, 2.24 mmol).

R_f: 0.5 (DCM: MeOH (15:1)).

^{1}H NMR (500 MHz, $CDCl_3$): δ 3.35 – 3.20 (bm, 10H, $4CH_2N$ & CH_2NH), 2.68 (bt, 2H, CH_2NH_2), 1.41 (s, 27H, $C(CH_3)_3$), 1.35 (s, 2H, NH_2).

2.3.5 Synthesis of Boc-tetramine-TEG-N_3 (5)

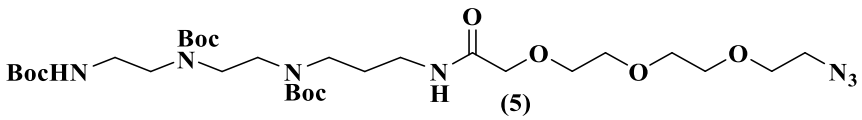

(5)

Compound 4 (150 mg, 0.3 mmol) and DIPEA 86 mg (0.67 mmol) were added to each other under argon conditions to initiate the reaction. In parallel to that, we added 86 mg (0.67 mmol) of DIPEA and 169 mg,(0.44 mmol) of TBTU into a solution of compound 3. And then, all of the solutions were added to 15 ml of acetonitrile. Afterward, the reaction was stirred at room temperature for 24 hours. On the next day, we added 70 ml of dichloromethane to the reaction and washed it with 30 ml of one molar of HCl. Then we separated the organic layer and dried it with sodium sulfate. The organic layer was evaporated under the vacuum by rotavap. DCM: MeOH (15:1) was used as a mobile phase to visualize the TLC. To purify the reaction, flash chromatography was used (DCM: MeOH (15:1)). Then, the yield was 89% (240 mg, 0.36 mmol).

R_f: 0.5 (DCM: MeOH (15:1)).

IR: 2105.28, 3345.60, 2928.01, 1688.25 cm^{-1}.

^{1}H NMR (500 MHz, $CDCl_3$): δ 3.96 (s, 2H, CH_2CONH), 3.68-3.64 (m, 8H, $4CH_2O$), 3.39-3.24 (m, 16H, $4CH_2N$, $2CH_2NH$, $COCH_2CH_2N_3$ & $COCH_2CH_2O$), 2.2 (t, 2H, J = 4.4 Hz, CH_2N_3), 1.44 (s, 27H, $C(CH_3)_3$).

2.3.6 Synthesis of MWCNTs-alkyne (6)

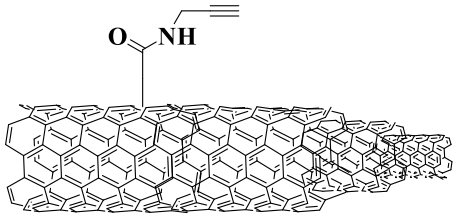

(6)

30 mg of carboxylated MWCNTs were dissolved in 30 ml of DMF. Then, 15.0 mg (0.08 mmol) of EDC and 150 µl (1.09 mmol) of Et3N were added. And after sonicating for an hour, we added (25 µl, 0.41 mmol) of propargylamine. Following sonication for 10 minutes, the mixture was stirred under argon for 72 hours. After three days, the reaction was diluted with 25 ml of CHCl3. Then, the reaction was filtered through a nano-filter under vacuum by using 20 ml of CHCl3 twice, 10 ml of DCM once, and finally 20 ml of diethyl ether twice. After the drying, we obtained 27 mg of black powder.

2.3.7 Functionalization of MWCNTs-Alkyne with compound 5 (7)

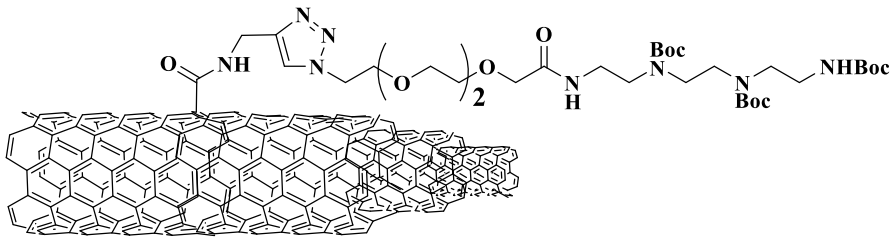

(7)

We dissolve 12 mg (0.07 mmol) of anhydrous CuSO4 and 5 mg (0.02 mmol) of solubilized L-ascorbic acid sodium salt in 5 ml of DW. The solution was added to a sonicated mixture of alkyne MWCNTs (6) 27 mg and compound (5) 100 mg (0.15 mmol) which was dissolved in 5 ml of DCM, and the reaction was stirred overnight. On the next day, we added 30 ml of methanol, and then the reaction was sonicated for 15

min. Then, the mixture was filtered by Nanofilters and the product was washed twice with methanol, and twice with diethyl ether. After drying the products in the oven, we obtained 25 mg of f-MWCNTs**.**

2.3.8 Deprotection *f*-MWCNTs 7 (8)

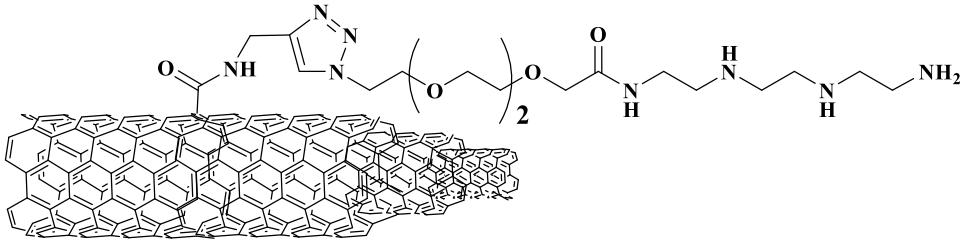

(8)

We took 25 mg of compound 7 (*f*-MWCNTs) which was dissolved in 5 ml of DCM and sonicated for 10 minutes. After that, 4 ml of TFA were added. Then, the reaction at room temperature was stirred overnight. On the next day, after repeated washings with MeOH and ether (2 x 30 ml each), black powder (23 mg) was obtained.

2.3.9 Synthesis of 4-aminophenyl α-D-mannopyranoside (9)

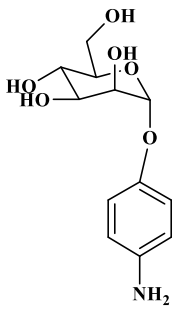

(9)

We dissolve 100 mg (0.37 mmol) of 4-nitrophenyl α-D-mannopyranoside in 5 ml of Milli Q water. After sonication for 10 minutes, we added 10 mg of Pd/C. Under bubbling H2 at room temperature, the reaction was stirred overnight. On the next day, we evaporated the water and added 10 ml of ethanol to facilitate removing the palladium.We take 27 mg of compound 6 (MWCNTs-alkyne) and 84 mg) (0.40 mmol) of compound 9, and then we disperse them in *o*-DCB:DMF 2:1 (25 ml) under the conditions of vacuum and argon. After 30 minutes of sonication under argon bubbling, 350 µl of iso-amyl nitrite was added to the reaction dropwise. Under argon, the reaction

was stirred at 65ºC for 24 hours. On the next day, the product was washed with methanol, aceton, and diethyl ether (2 x 30 ml each), and then 25 mg of black powder was obtained after drying

2.3.11 Functionalization of *f*-MWCNTs (10) with compound 5 (11)

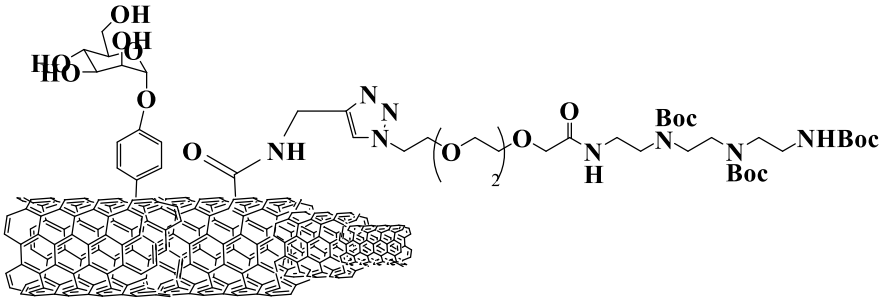

(11)

We dissolve 12 mg) (0.07 mmol) of anhydrous CuSO4 and 5 mg (0.02 mmol) of Solubilized L-ascorbic acid sodium salt in 5 ml of DW. The solution was added to a sonicated mixture of alkyne-mannose MWCNTs (6) 28 mg and compound (5) 100 mg (0.15 mmol), which was dissolved in 5 ml of DCM, and the reaction was stirred overnight. On the next day, we added 30 ml of methanol, and then the reaction was sonicated for 15 min. Then, the mixture was filtered by nanofilters and the product was washed twice with methanol, and twice with diethyl ether. After drying the products in the oven, we obtained 25 mg of *f*-MWCNTs**.**

2.3.12 Deprotection of *f*-MWCNTs 11 (12)

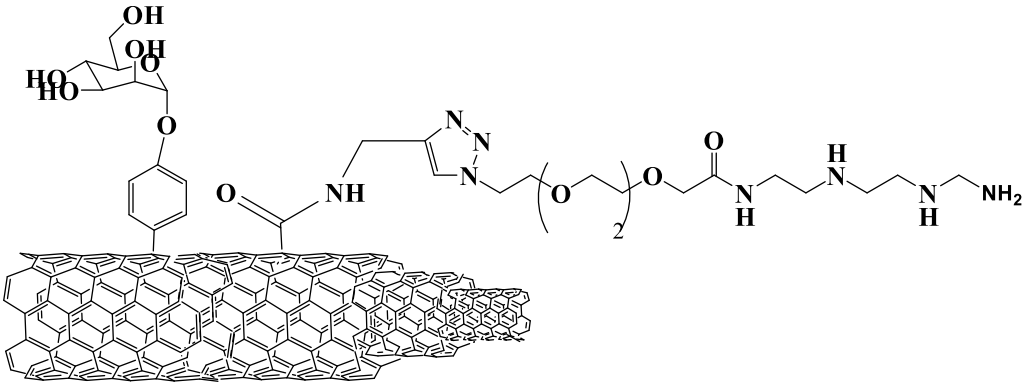

(12)

We took 25 mg of compound 11 (*f*-MWCNTs) which was dissolved in 5 ml of DCM and sonicated for ten minutes. After that, 4 ml of TFA were added. Then, the reaction at room temperature was stirred overnight. On the next day, after repeated washings with methanol and ether (2 x 30 ml each), black powder (23 mg) was obtained.

2.3.12 Quantification of the amounts of free-loaded amine on carbon nanotubes by Kaiser test protocol [109]

1. **Separate solutions were prepared for each of the following:**
    - 40.0 grams of phenol in 10 ml of absolute ethanol (solution number I).
    - 2 ml of 1 mM potassium cyanide (KCN) in 98 ml of pyridine 1 mM of potassium cyanide was prepared by adding 65 KCN to 100 ml of DW (solution number II).
    - One gram of ninhydrin in 20 ml of absolute ethanol (solution number III).

Procedure:

First of all, we used an Eppendorf to weigh 1.2 mg of different types of carbon nanotubes (i.e: MWCNTs (blank 1), *f*-MWCNTs with a tetra-amine linker, and *f*-MWCNTs with mannose and a tetra-amine linker). Then, 75 µl of solution (I), 100 µl of solution (II), and 75 µl of solution (III) were added to each Eppendorf of carbon nanotubes. After that, all Eppendorf were sonicated for 5-10 minutes. Then, we cooked the Eppendorf at 120 °C for 10 min. Finally, after cooling the Eppendorf's, all of them were diluted by adding 1 ml of 60% ethanol, then we filtrated them with a glass dropper, and then the tube was washed with another 1 ml of 60% ethanol. In the following step, the filtrate was analyzed by UV-Vis spectroscopy at λ 570 nm to determine how many amines were functionalized on CNTs using this equation:

$$\mathbf{NH_2\ Loading\ (mmol/mg)} = \frac{\mathbf{[Abs_{sample} - Abs_{blank}] \times dilution\ (ml) \times 10^3}}{\mathbf{Extinction\ coefficients \times Sample\ weight\ (mg)}}$$

A dilution of 2.25 ml has been used, and the extinction coefficient is 15000 M-1 cm-1. In addition, we expressed our results in mmol of amine groups per gram of CNT.

2.3.13 Determination of the loaded amounts of mannose sugar in the carbon nanotubes by anthrone method [110, 111]

1. Spectrophotometric calibration curve for mannose

Mannose calibration curves were prepared using serial dilutions (0.01, 0.02, 0.03, 0.04, 0.05 mg/ml) of (1 mg/ml) mannose in DW at λmax 620 nm.

2. Anthrone method

We took 0.5 ml from each dilution and added each one of them to 1 ml of anthrone solution (0.2% anthrone in sulfuric acid) at 0 ºC. Then, the samples were incubated for 10 minutes at 100 ºC. In the following step, the samples were cooled to room temperature. In the end, 620 nm was chosen as the wavelength of maximum absorbance.

2.4 Gel electrophoresis to determine the best N/P ratio

2.4.1 Composition of FA gel buffers

Table 1

Composition of FA gel buffers

1.	10x FA gel buffer	41.46 g MOPS 6.8 g sodium acetate 2.9 g EDTA Up to 1000 ml of distilled water pH 7.0 with NaOH
2.	1x FA gel buffer	100 ml 10x FA gel buffer 20 ml 37% formaldehyde (12.3 M) Up to 1000 ml RNase-free water
3.	5x RNA loading buffer	16 µl saturated aqueous bromophenol blue solution 80 µl EDTA (500 mM) (EDTA solution adjusted previously with NaOH to pH 8.0) 720 µl 37% formaldehyde (12.3 M) 2 ml 100% glycerol 3084 µl formamide 4 ml 10x buffer Up to 10 ml RNase-free water

2.4.2 Formaldehyde agarose gel

We added 1.2 g of agarose to 10 ml of 10x FA gel buffer, followed by RNase-free water to 100 ml. Agarose was melted in a microwave and then cooled to 65°C. Then, 1.8 ml of 37% formaldehyde was added. We then poured the warm solution into an appropriate gel cassette and inserted combs to form wells. After 30 minutes of polymerization, the agarose gel was immersed for at least 30 minutes in 1x FA gel running buffer.

2.4.3 Samples preparation, loading, and running for *f*-MWCNTs (8) and *f*-MWCNTs (12)

We estimated the N/P ratio based on Kaiser test results for our compounds.

- The first thing we prepared was a stock solution for each compound. For *f*-MWCNTs (8) we made a stock of 2 mg/mland 1 mg/1.5ml for *f*-MWCNTs (12). In addition, the stocks were functionalized non-covalently with 1 ml of 5 % Tween 20. Moreover, the excess amounts of TWEEN 20 were removed by membrane dialysis overnight.
- N/P ratio means that the micromolar of the amine group (μM -amine) to the micromolar of the phosphate group (μM –phosphate).
- The amount of amine in *f*-MWCNTs (8) is 0.0127 mmol/mg = 12.7 μmol/mg = 12.7 x 103 nmol/mg. While the amount of amine in *f*-MWCNTs (12) is 0.04 mmol/mg = 40 μmol/mg = 40 x 103 nmol/mg.
- A 2 mg/ml of *f*-MWCNTs (8) contains (2 x 12.7 x 103 nmol/1ml) which equals 25.4 nmol/μl. And 1 mg/1.5 ml of *f*-MWCNTs (12) contains (26.6 x 103 nmol/ml) which equals 26.6 nmol/μl.
- Also, we need to know that for each 1 μl of β-catenin siRNA we have 10 μM phosphate. While in each 1 μl of our stocks we have 25.4 μM of amine in *f*-MWCNTs (8) and 26.6 μM of amine in *f*-MWCNTs (12).
- For example, take 2.5/1 as the N/P ratio, this ratio means that 2.5 μM –amine / 1 μM –phosphate and it equal to (25 μM –amine: 10 μM –phosphate). So to achieve a 2.5/1 N/P ratio we need 1 μl of *f*-MWCNTs –amine & 1 μl of siRNA. Also, 5/1 needs 2 μl of *f*-MWCNTs –amine and 1 μl of siRNA. Also for *f*-MWCNTs (12) as well, take 2.5/1 as the N/P ratio, this ratio means that 2.5 μM –amine / 1 μM –phosphate and is equal to (25 μM –amine: 10 μM –phosphate). So to achieve a 2.5/1 N/P ratio we need 1 μl of *f*-MWCNTs –amine & 1 μl of siRNA. Also, 5/1 needs 2 μl of *f*-MWCNTs –amine and 1 μl of siRNA.

- From these data, we can calculate the other N/P ratios, and it will be like the following:

Table 2

Sample composition for each N/P ratio in f-MWCNTs (8)

N:P ratio (μM)	*f*-MWCNTs-amine (μl)	siRNA (μl)	5X buffer (μl)	Novel juice (μl) (Nucleic acid stain)
10:1	4	1	1.25	2
7.5:1	3	1	1	2
5:1	2	1	0.75	2
2.5:1	1	1	0.5	2
1.25:1	0.5	1	0.25	2
0.625 : 1	0.25	1	0.125	2

Table 3

Sample composition for each N/P ratio in f-MWCNTs (12)

N:P ratio (μM)	*f*-MWCNTs-amine-mannose (μl)	siRNA (μl)	5X buffer (μl)	Novel juice (μl) Nucleic acid stain)
15:1	6	1	1.75	2
12.5:1	5	1	1.5	2
10:1	4	1	1.25	2
7.5:1	3	1	1	2
5:1	2	1	0.75	2
2.5:1	1	1	0.5	2
1.25:1	0.5	1	0.25	2

- After we prepared the sample, the samples were incubated for 20min at room temperature, and then we loaded them into the gel wells. The electrophoresis was run using 1x FA gel buffer at 70 V for 30 min.

2.5 Semiquantification of beta-catenin protein expression by immune blot for *f*-MWCNTs (8) (*f*-MWCNTs –amine).

2.5.1 Immunoblotting Buffers and anti-bodies solution

Table 4

Immunoblotting Buffers and anti-bodies solution preparations amounts

1.	GST-fish buffer (500 ml)	25 ml 1 M Tris (pH 7.4 with HCl) 75 ml 1 M NaCl 2 ml 1 M MgCl2 50 ml glycerol 5 ml Igepal CA-630 up to 500 ml distilled water
2.	4x SDS-PAGE sample loading buffer without glycerol (50 ml)	5 ml β-mercaptoethanol 3.25 g SDS 15 ml 300 mM Tris (pH 6.8 with HCl) 0.125 g bromophenol blue up to 50 ml of distilled water
3.	10x TBS buffer (1000 ml)	12.12 g Tris 87.65 g NaCl up to 1000 ml of distilled water pH 7.4 with HCl
4.	TBS-T buffer (1000 ml)	1000 ml 10x TBS 1 ml tween 20
5.	5x SDS-PAGE electrophoresis buffer (1000 ml)	15.1 g Tris 94 g glycine 5 g SDS up to 1000 ml of distilled water pH 8.3 with KOH
6.	Blotting buffer (1000 ml)	3.02 g Tris 14.4 g glycine 200 ml methanol up to 1000 ml distilled water
7.	10% Ammonium persulfate (APS), (10 ml)	1 g APS up to 10 ml of distilled water
8.	10% SDS (100 ml)	10 g SDS up to 100 ml of distilled water
9.	1.5 M Tris pH 8.8 (100 ml)	18.15 g Tris base Up to 100 ml of distilled water pH 8.8
10.	1 M Tris pH 6.8 (100 ml)	12.11 g Tris base Up to 100 ml of distilled water pH 6.8
11.	1x Roti-ImmunoBlock	1 ml 10x Roti-ImmunoBlock 9 ml distilled water
12.	Beta-catenin anti-body (primary antibody)	2 µL in 10 ml TBST (1: 5000)
13.	Beta-actin antibody (primary antibody)	10 µL in 10 ml TBST (1: 1000)
14.	2^{o} anti-body (anti-mouse peroxidase antibody)	1 µL in 10 ml TBST (1: 10,000)

2.5.2 Cell culture

The first step in cell culture was the culturing of the Caco-2 cells in T-175 cell culture flasks containing RPMI basal medium supplemented with L-glutamine (1%), FBS (10%), and penicillin/streptomycin (1%). At 37°C, 5% CO2, and 99% humidity, the cells were kept in a standard cell culture incubator.

After 72 hours, the medium was suctioned and washed with Ca2+-free PBS before subculturing. Following that, cells were incubated in the incubator with 0.025% trypsin for 5 minutes until sufficient cells detached from the flask. Then, CGM was used to inactivate the trypsin, then the cell suspension was collected, and a trypan blue stain was used to determine the viable cell count before adjusting the cell concentration.

2.5.3 Cell preparation for transfection

Caco-2 cell suspension was prepared in a serum-free, antibiotic-free medium. After trypsin inactivation with serum-containing medium, the cells were collected and the living cells were counted, then they were spun down at 150 g for 7 min, the supernatant was completely removed, and the cells were re-suspended in serum-free and antibiotic-free medium so that the cell concentration was 300,000 cells/ml (based on the cell count).

2.5.4 Transfection Complex preparation.

Nine µL of Lipofectamine RNAiMAX reagent were diluted with 150 µL medium (containing no serum or antibiotic). In parallel, 10 µL siRNA (10 µM) was diluted with 150 µL medium (no serum, no antibiotic). Then the diluted siRNA was added to the diluted Lipofectamine RNAiMAX (1:1 ratio).

Moreover, 5 µL of *f*-MWCNTs (8) werediluted with 150 µL medium (containing no serum or antibiotic). In parallel, 10 µL siRNA (10 µM) was diluted with 150 µL medium (no serum or antibiotic). Then the diluted siRNA was added to the diluted *f*-MWCNTs (8) (1:1 ratio).

Then the mixtures were incubated for 20 min at room temperature. The transfection mixture (300 µL) of either Lipofectamine with siRNA or *f*-MWCNTs (8) with siRNA was transferred to a well of a 12-well plate, then 2 ml of cell suspension (300,000

cells/ml) was added to the well, gently mixed and, the plate was incubated for 4 hr. After that, 250 µl serum, 25 µl antibiotic stock, and 1 ml complete medium were added, and incubated overnight. A similar control sample will be prepared with the same procedure but without adding siRNA. We had two control groups, the first one was lipofectamine without siRNA, and the second one was *f*-MWCNTs (8) without siRNA.

2.5.5 Protein sample preparation

The medium must first be aspirated, then two washes with PBS were performed, and the cells were lysed with ice-cold GST-fish lysis buffer (400uL) using cell scrapers. Cells scraped from the plates were centrifuged for 5 minutes at 13000 g to remove debris, followed by the addition of 1:4 of the 4x sample loading buffer containing no glycerol to the supernatant. Incubation was conducted at 95ºC for 5 minutes on a heating block shaker, followed by cooling on ice, followed by centrifugation and cooling until use. SDS-gel should be loaded after gentle mixing and centrifugation. Additionally, a protein sample of 30-35 uL will be loaded into each well of the SDS-gel.

2.5.6 SDS-polyacrylamide gel

Table 5

5% and 12% SDS-polyacrylamide gel preparation amounts

12 % SDS-polyacrylamide gel (25 ml)	10.75 ml distilled water 7.5 ml 40% acrylamide rotiphorese gel solution 6.25 ml 1.5 M Tris pH 8.8 250 uL 10% SDS 250 uL 10% APS 12.5 uL TEMED
5% SDS-polyacrylamide gel (10 ml)	3.625 ml distilled water 650 uL 40% acrylamide rotiphorese gel solution 625 uL 1.5 M Tris pH 8.8 50 uL 10% SDS 50 uL 10% APS 5 uL TEMED

2.5.7 Immunoblotting

Protein samples mixed with a loading buffer were loaded on a 5% SDS-polyacrylamide gel layer. 70 minutes were needed to run the electrophoresis at 200 volts. Immediately following the gel blotting, the proteins are blotted onto nitrocellulose membranes with

100 volts under cooled conditions. To visualize the protein markers on the membrane, the nitrocellulose membranes were then stained with Ponceau S stain for 5 minutes at room temperature. Multiple washes of distilled water were used to remove excess dye, and membranes were cut based on the protein marker so that different primary antibodies could be incubated. A series of TBS-T washes and a 1x Roti-block incubation at room temperature for an hour destain the membranes.

After that, a series of three washes with TBS-T were conducted, each lasting 5 minutes, followed by overnight incubation with primary antibodies at 4°C. After 24 hours, we then washed the membranes three times with TBS-T each for five minutes and incubated them for one hour at room temperature with shaking with HRP-conjugated secondary antibodies. After that, three times with TBS-T were then used to wash the membranes, each for 5 minutes, and at the end, we visualized protein antibody complexes using the Versa doc MP detection system using either Lumi-light western blotting substrate kit.

Figure 2.1

Steps for performing a westren blot

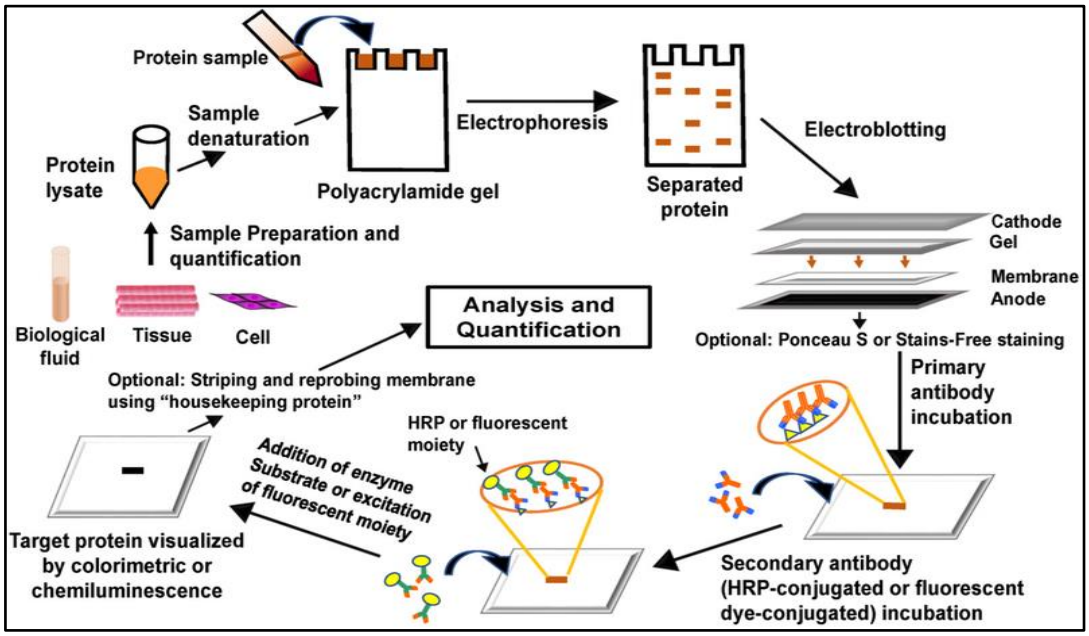

Mishra, M., S. Tiwari, and A.V. Gomes, Protein purification and analysis: next generation Western blotting techniques. Expert review of proteomics, 2017. **14**(11): p. 1037-1053.

2.6 Semiquantification of beta-catenin protein expression by immune blot for *f*-MWCNTs (12) (*f*-MWCNTs –amine & mannose), and *f*-MWCNTs with Tween 20.

Before quantifying the amounts of knock-down of β-catenin proteins by f-MWCNTs (8)-siRNA, we prepared immunoblotting buffers and cultured the Caco-2 cell line, and prepared the Caco-2 cells for transfection as mentioned previously. Then, we transfected the cells with lipofecatamine-siRNA as mentioned previously. Furthermore, 5 µL of CNT-TWN were diluted with 150 µL medium (containing no serum or antibiotic).

In parallel 10 µL siRNA (10 µM) was diluted with 150 µL medium (no serum or antibiotic). Then the diluted siRNA was added to the diluted *f*-MWCNTs -Tween 20 (1:1 ratio). Moreover, 60 µL of *f*-MWCNTs (12) was diluted with 150 µL medium (containing no serum, no antibiotic). In parallel 10 µL siRNA (10 µM) was diluted with 150 µL medium (no serum or antibiotic). Then the diluted siRNA was added to the diluted *f*-MWCNTs (12) (1:1 ratio). Then the mixtures were incubated for 20 minutes at room temperature.

The transfection mixture (300 µL) of Lipofectamine with siRNA, *f*-MWCNTs (12), and *f*-MWCNTs –Tween 20 was transferred to a well of a 12-well plate, and then 2 ml of cell suspension (300,000 cell/ml) were added to the well. The mixture was gently mixed and the plate was incubated for 4 hrs. After that, 250 µl serum, 25 µl antibiotic stock, and 1 ml of complete medium were added and incubated overnight. A similar control sample will be prepared with the same procedure but without adding siRNA. We had three control groups, the first was lipofectamine without siRNA, the second was *f*-MWCNTs (12) without siRNA, and finally *f*-MWCNTs –Tween 20 without siRNA. After 48 hours of transfection, we prepared protein samples and did a western blot as mentioned previously.

2.7 Cell growth and anti-cancer activity of 5-FU

In order to access the anti-cancer activity of the 5-FU we cultured the Caco-2 cells followed by transfection with lipofectamine, f-MWCNTs (8), and f-MWCNTs (12) complexed with siRNA as previously described. After 24 hours of transfection, the transfected cells with β-catenin siRNA by different approaches were sub-cultured in the 96-well plate at 5000 cells per well.

The cells were then allowed to adhere and accommodate overnight before tests were conducted. On the next day, we added 20 µl of MTS reagent to each well and incubated them for 2 hours in the incubator. And after that time, we measured the absorbance at 490 nm using the pleat reader. Also, in the other 96 well plates with the same procedures for transfection and sub-culture, we prepared different concentrations of 5-FU, which are 500 µg/ml, 250 µg/ml, 125 µg/ml, and 62.5 µg/ml under a 7.4 pH condition. After that, we add 100 µl of each concentration to each well after 48 hours of transfection. After 48 hours, we add 20 µl of MTS reagent to each well and incubate it for 2 hours in the incubator. After that time, we measured the absorbance at 490 nm by using the pleat reader.

Chapter Three

Results and Discussion

3.1 Synthesis and functionalization of MWCNTs

siRNA is a double-stranded non-coding regulatory ncRNA that has a negative charge. In order to deliver this molecule inside the cancer cells formation of chemical interaction with the positive group is needed. Several experiments used the tetra-amine group that has a positive charge to form ionic interaction with the negative phosphate group of the siRNA [112]. Moreover, the addition of mannose molecules can improve the transfection amounts and efficacy [113].

This research aims to develop a new nanosystem of functionalized MWCNTs with a tetra-amine linker and mannose sugar via a covalent bond. A tetra-amine linker was loaded to the MWCNTs to enhance their biocompatibility and dispersibility in water on the one hand and to form a complex with β-catenin siRNA via electrostatic interaction on the other hand. Also, we added mannose sugar as a targeting agent to increase the nanosystem selectivity in cancer cells. Consequently, the nano-system became able to deliver the β-catenin siRNA selectively and efficiently into cancer cells.

The following section describes the results of the synthesis of the tetra-amine linker and how MWCNTs get functionalized. To begin with, we connected the MWCNTs with amine moieties via a derivative of tetraethylene glycol (TEG). Several steps were used to synthesize the derivatives of TEG.

First of all, the reaction started with the reaction of the OH moiety of the tetra-ethylene glycol with tosyl group to form a compound number (1). In the next step, by using sodium azide in ethanol, the tosyl group of compound (1) was then replaced with an azide group to obtainOH-TEG-N_3 (compound 2). Furthermore, compound (2) underwent an oxidation reaction to get COOH-TEG-N_3 (compound 3), as illustrated in Scheme B.

Scheme A

Synthesis of Tetraethylene glycol derivative linker (COOH-PEG-N3)

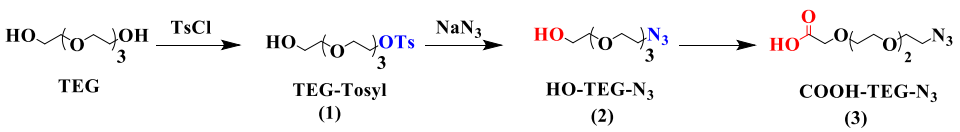

Upon synthesizing linker (3), which is the part of the linker related to the functionalized MWCNTs dispersibility and biocompatibility. The tetraamine spacer was consequently added to compound (3) in this manner. Starting with selective Boc group protection of three amine moieties in tetraamine, we got compound (4). Using TBTU as a coupling agent and DIPEA as a base, the Boc-protected tetraamine spacer was reacted with compound (3) to yield compound (5), as we see in Scheme C.

Scheme B

Synthesis of compound (5)

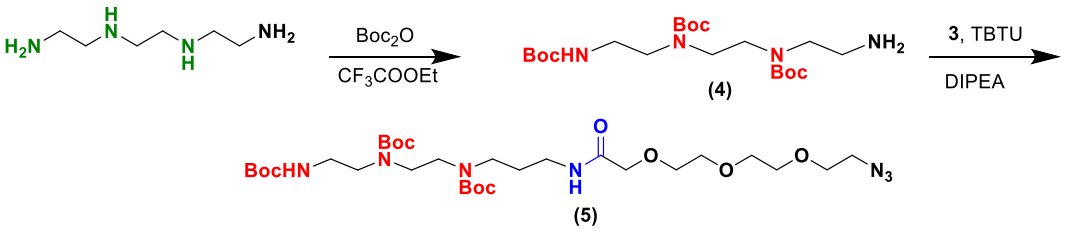

Compound (5) is then attached to the MWCNTs. An amidation reaction was performed on the carboxylated-MWCNTs to generate terminal alkyne moiety on the top of MWCNTs (6**)**. The click reaction in DCM: H2O (1:1) using copper sulfate and ascorbic acid between compound (5) and *f*-MWCNTs was then carried out to obtain compound (8). Under acidic conditions, the Boc group was removed with TFA to obtain the tetramine spacer in the MWCNTs (9), as we see in Scheme D.

Scheme C

Functionalization of MWCNTs with alkyne and tetra-amine linker

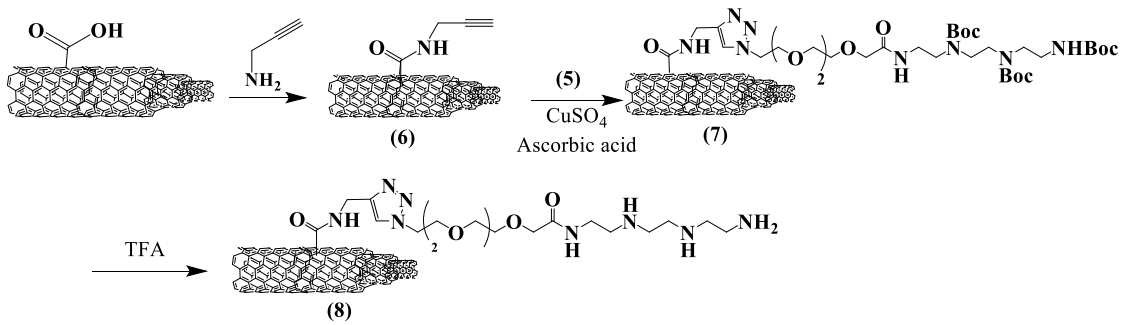

After the functionalization of MWCNTs with tetra-amine linker and to specifically target cancer cells, we functionalized the MWCNTs with tetramine spacers and mannose as targeting agents. As we mentioned previously, many cancer cells, such as colorectal cancer cells, breast cancer cells, etc, can overexpress mannose receptors on

their surface [114]. Accordingly, and to attain this aim, we produced 4-aminophenyl α-D-mannopyroinoside from a reduction of 4-nitrophenyl α-D-mannopyroinoside in the presence of palladium and hydrogen gas (9), as we see in Scheme 2.D. Then the 4-aminophenyl α-D-mannopyroinoside was bonded to MWCNTs via diazonium reaction or also called tour reaction, as we see in Scheme E.

Scheme D

Synthesis of 4-aminophenyl α-D-mannopyroinoside

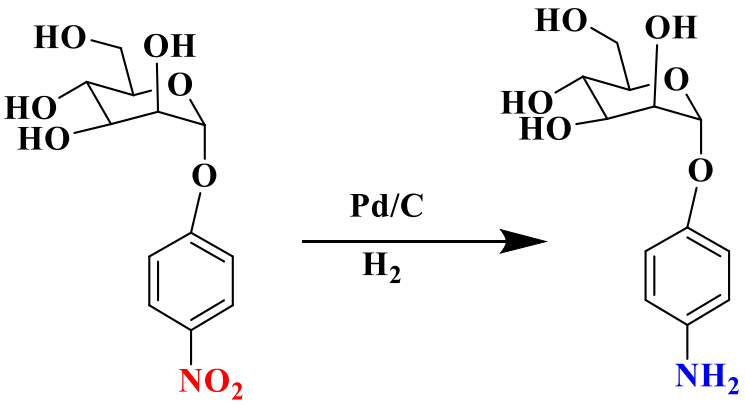

(9)

By using iso-amyl nitrite as a catalyst, compound (9), which was used in the reaction with *f*-MWCNTs (6), a reaction called tour reaction was converted the *f*-MWCNT (6) to compound (10**)**. Then, a click reaction was then conducted between the *f*-MWCNTs (10) and compound (5) with catalysts which are ascorbic acid and anhydrous $CuSO_4$ dissolved in DCM and water to obtain the *f*-MWCNTs (11). In Scheme F, you can see the functionalized MWCNTs (12) after removing the Boc group under acidic conditions using TFA.

Scheme E

Functionalization of MWCNTs with tetra-amine linker and mannose sugar

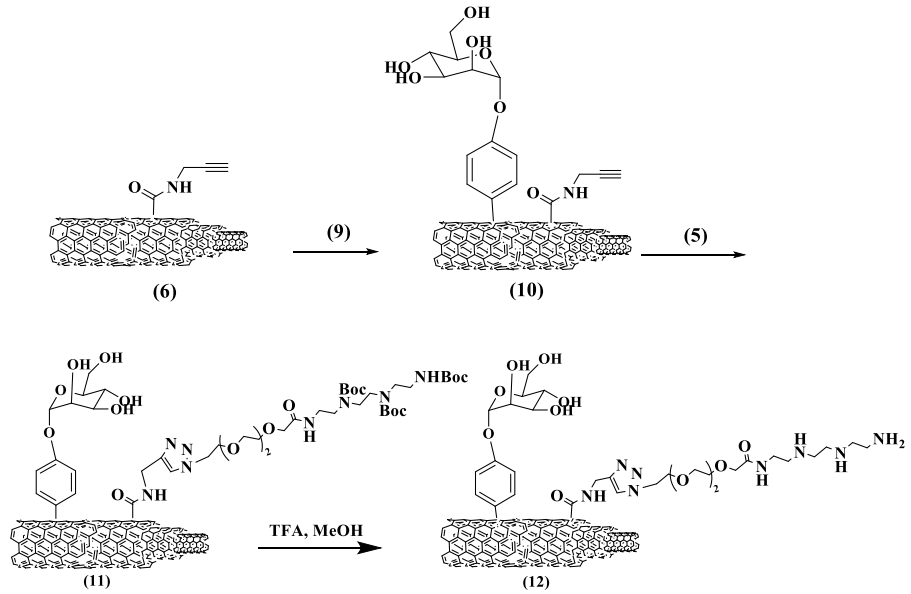

3.2 Characterization of *f*-MWCNTs

3.2.1 AFM images of the *f*-MWCNTs and their dispersibility

To study the morphology of carbon nanotubes, an atomic force microscope (AFM) was used to study this feature in the functionalized MWCNTs. AFM is a powerful tool that images and measures surfaces at the nanoscale. An AFM technique involves probing a sample's surface using a sharp tip attached to a cantilever, which is attached to a sharp tip. AFM works by bringing the tip close to the sample surface. Then, the tip's position is controlled using a feedback mechanism. When the tip contacts the sample surface, the cantilever bends by an optical detector to detect the bending. This is done through the reflection of a laser beam off the cantilever's back. The detector measures the laser beam deflection and provides information on the sample's height and surface morphology [115].

As we see in figure 3.A1 (A), the carbon nanotubes aggregated on each other. and they appeared as bundles of tubes due to Vander Walls interaction between the aromatic rings of the carbon tubes. They precipitated immediately. While in Figures 3.A1 (B) and 3.A1 (C), or after mono and di-functionalization of MWCNTs, the dispersibility of carbon nanotubes increased, and they appeared as separate tubes due to repulsive forces between them due to the functionalization with a diameter range of 5-10 nm. Moreover,

as can be observed in the vials of figure 3.1B and C, the *f*-MWCNTs 8 and 12 are totally dispersed in water.

Figure 3.A1

Vigulization of f-MWCNTs by FAM

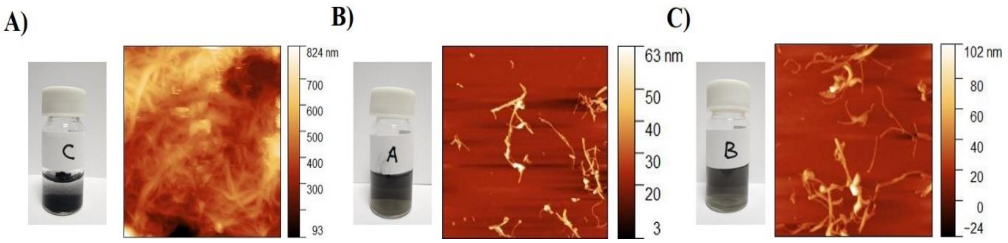

AFM image of A) non-functionalized MWCNTs, B) f-MWCNTs with a tetraamine linker (8), and C) dual functionalization of MWCNTs with a tetraamine linker and mannose sugar (12).

3.2.2 UV-Vis spectrophotometry

3.2.2.1 Determination of the loaded amine on *f*-MWCNTs

A Kaiser test was conducted to determine the loaded amine amounts on *f*-MWCNTs with amine (8) and *f*-MWCNTs with amine and mannose (12). The loaded amine in *f*-MWCNTs (8) was 12.7 * 10^3 nmol/mg and 40 * 10^3 nmol/mg in *f*-MWCNTs (12). The loaded amine obtained in both *f*-MWCNTs (8) and *f*-MWCNTs (12) is considered a large amount compared to other experiments that can prove the ability of MWCNTs to load large amounts of molecules on their surface [112].

3.2.2.2 Calibration curve of Mannose

The expression of receptors on the surface of cancer cells is an important feature that can be invested to increase the targeting and selectivity of nanoparticle-based therapy. Functionalization of CNTs with mannose molecules is one of the newest approaches to increase the targeting and loading of CNTs to cancer cells especially when the loaded amount is high.

So, after the functionalization of MWCNTs with mannose sugar we used the anthrone methods to measure the loaded amounts of mannose. Also, a calibration curve was obtained for mannose at λmax = 620 nm, and $R^2$was 0.9967, (Figure 3.A2). The loaded amount of mannose on compound (12) was 20.02 µg/mg which is a high loaded amount of mannose compared with previous experiments [113].

Figure 3.A2

A calibration carve of mannose at λmax=620nm

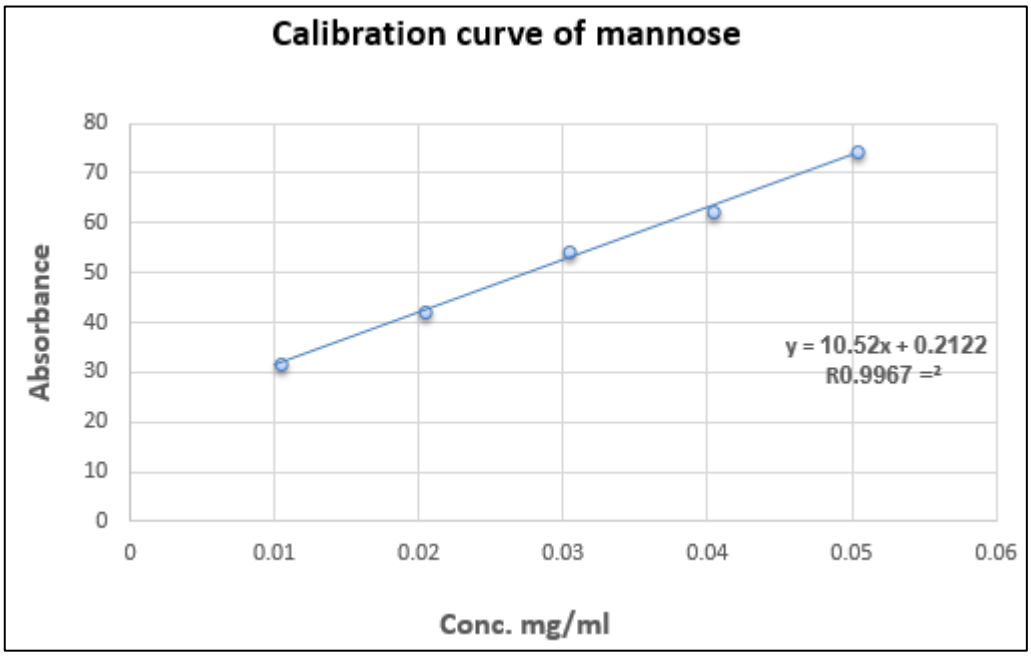

3.3 Gel electrophoresis to determine the optimum N/P ratio

3.3.1 Estimation of *f*-MWCNTs (8)-siRNA complex formation.

f-MWCNTs (8)-siRNA complex formation was investigated using agarose gel electrophoresis at various N/P ratios (0.625/1, 1.25/1, 2.5/1, 5/1, 7.5/1, and 10/1). The complex formation can be confirmed by observing a retarded migration of siRNA in an agarose gel. In addition, since the siRNA must be released into the cells to have a chance to interact with mRNA there, the *f*-MWCNTs (8)-siRNA complex formation must be reversible. As can be observed in figure 3.B, the 1.25/1 ratio (equal to 0.5 µl of *f*-MWCNTs: 1 µl siRNA) is considered the minimum ratio that prevents the full amount of siRNA from migrating out of the wells on the agarose gel by forming large complexes that cannot pass through the pores of the gel.

Figure 3.B

Determination the best N/P ratio for f-MWCNTs (8) by agarose gel electrophoresis

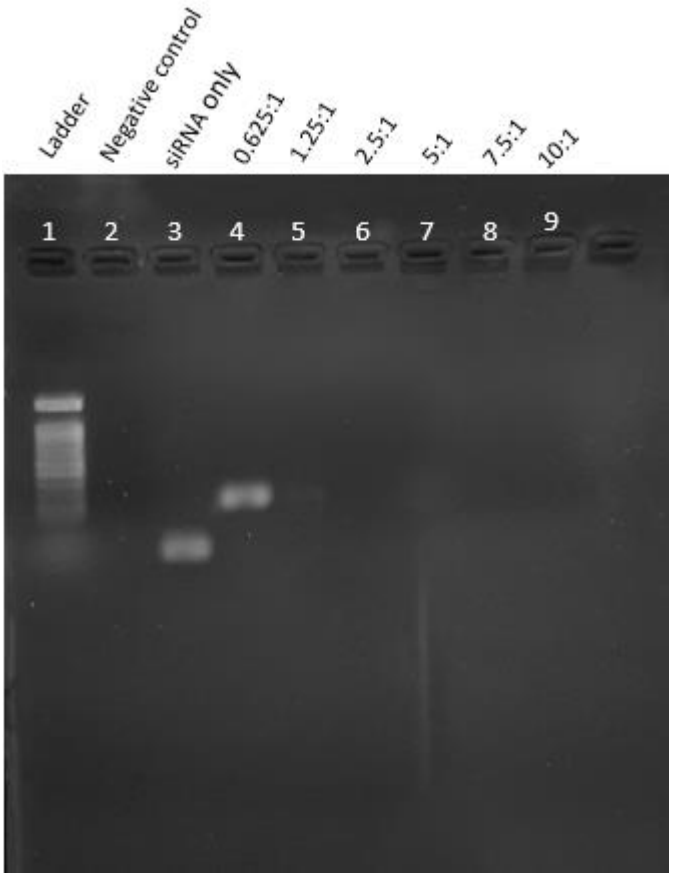

Determination of the optimum N/P ratio via agarose gel electrophoresis subjected to UV light to visualize the free siRNA in the (1) ladder, (2) negative control (MWCNT-NH2 only), (3) siRNA only, (4) 0.625/1, (5) 1.25/1, (6) 2.5/1, (7) 5/1, (8) 7.5/1, and (9) 10/1

3.3.2 Estimation of *f*-MWCNTs (12)-siRNA complex formation

As in 3.2.1, we investigated the *f*-MWCNTs (12)-siRNA complex formation via agarose gel with different N/P ratios, which are (1.25/1, 2.5/1, 5/1, 7.5/1, 10/1, 12.5/1, and 15/1). And as we see in figure 3.C, the 15/1 ratio, which is equal to 6 µl of *f*-MWCNTs and 1 µl siRNA, is considered the minimum ratio that can trap the full amount of the siRNA molecules in the wells of the gel. We can hypothesize that the reason for this relatively low ratio is the presence of mannose sugar which might work as a steric hindrance.

As shown previously, the loaded amount of mannose is much higher than the loaded amount of amine. Consequently, it can be proposed that the repulsion forces between the OH moieties in the mannose sugar and the phosphate moieties of the siRNA could

be stronger than the attraction forces between the amine moieties in the tetraamine linker and the phosphate moieties of the siRNA. In our ratio, the amount of *f*-MWCNTs (12) that was used in each transfection is 60 µl which is a biocompatible amount of *f*-MWCNTs.

Figure 3.C

Determination the best N/P ratio for f-MWCNTs (12) by agarose gel electrophoresis

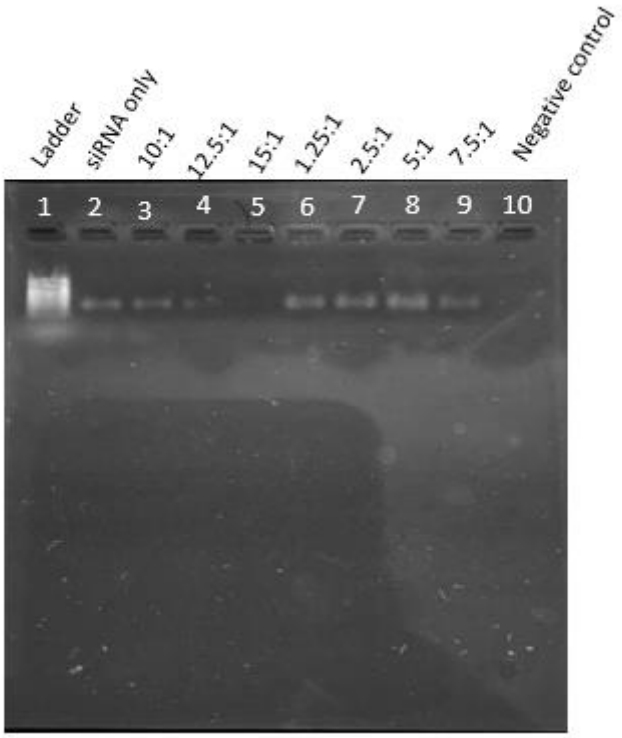

Determination of optimal N/P ratio via agarose gel electrophoresis subjected to UV light to visualize the free siRNA in the (1) ladder, (2) siRNA, (3) 10/1, (4) 12.5/1, (5) 15/1, (6) 1.25/1, (7) 2.5/1, (8) 5/1, (9) 7.5/1, and (10) negative control (MWCNTs-amine & mannose)

3.4 Knockdown of β-catenin

3.4.1 Knockdown of β-catenin by siRNA delivered by Lipofectamine and *f*-MWCNTs (8)

After transfection of siRNA by Lipofectamine and *f*-MWCNTs (8) into Caco-2 cells, as explained previously, the cell's contents of proteins were collected and processed. Then, we did a western blot, and the membrane was imaged by Azure Biosystems, Inc. In addition, ImageJ software was used to analyze the band density. After that, compared to the band of the housekeeping gene β-actin, the density of the β-catenin bands on the

membrane was reduced by around 30% by lipofectamine, 20% by *f*-MWCNTs (8), as we see in figure 3.D**.**

Figure 3.D

Western blot results for *β-catenin protein after 48 hour of transfection by f-MWCNT*

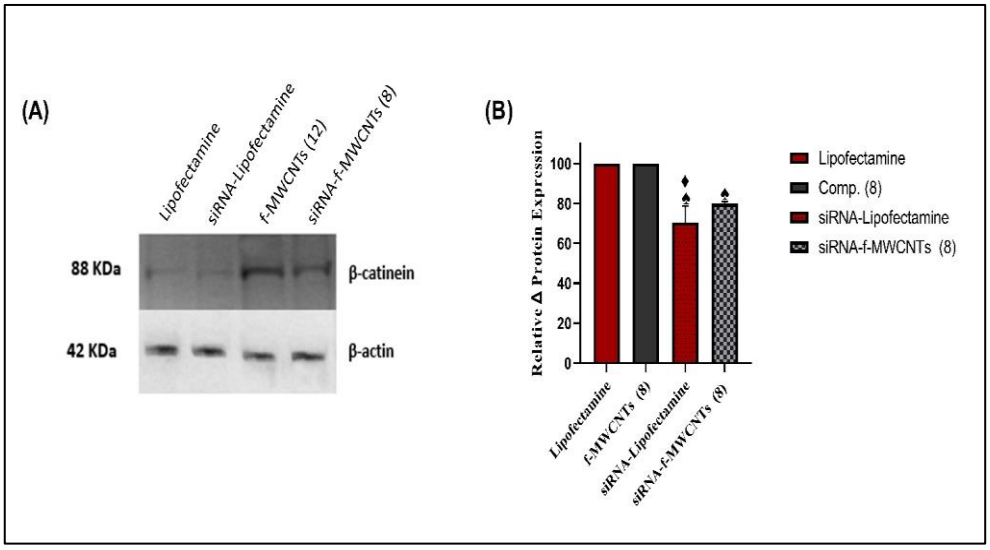

siRNA specific for β-catenin was transfected into Caco-2 cancer cells via both Lipofectamine and f-MWCNTs (8) to assess the relative change expression of the β-catenin protein. (A) Western blot results of negative control (1) group (lipofectamine only), transfected group via β-catenin siRNA complexed with lipofectamine, negative control (2) group (f-MWCNTs (8) only) and transfected group via β-catenin siRNA complexed with f-MWCNTs (8). (B) the β-catenin protein expression was significantly decreased in both transfected approaches compared with control. ♠Pv<0.05 compared to the control. ♦Pv<0.05 compared between others species. And all the data were analyzed by a one-way ANOVA test

3.4.2 Knockdown of β-catenin by siRNA delivered by Lipofectamine, *f*-MWCNTs (12) and CNT-TWN.

After transfection of siRNA by Lipofectamine, *f*-MWCNTs (12), and CNT-TWN 20 in Caco-2 cells, as explained previously, the cells' contents of proteins were collected and processed. Then, we did a western blot, and the membrane was imaged by Azure Biosystems, Inc. In addition, ImageJ software was used to analyze the band density. As shown in figure 3.E, the density of the β-catenin bands was reduced by around 30% by lipofectamine and 50% by *f*-MWCNTs (12). We hypothesize that the increase in transfection efficacy could be attributed to a possible up regulation of mannose receptors on the surface of the Caco-2 cells, which highlights the potential of the mannose sugar as a targeting agent and its role in delivering siRNA by our nanosystem [114]. On the other hand, the β -catenin knockdown did not happen at all, which

indicates that the functionalization of our compounds with Tween 20, which was done in order to increase the compound's dispersibility and solubility, does not form any type of interaction with the siRNA.

Figure 3.E

Western blot results for *β-catenin protein after 48 hour of transfection by f-MWCNT*

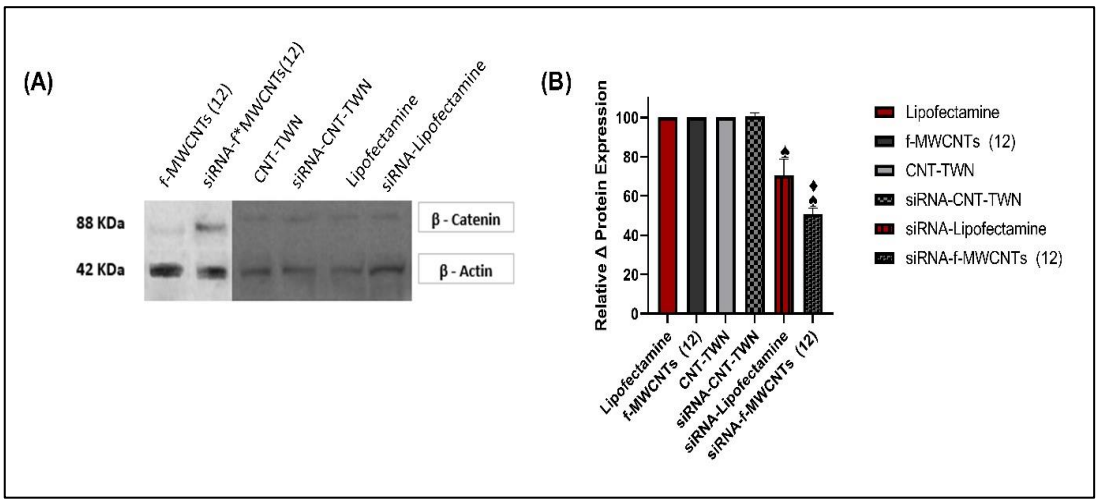

siRNA specific for β-catenin was transfected into Caco-2 cancer cells via Lipofectamine, CNT-TWN, and f-MWCNTs (12) to assess the relative change expression of the β-catenin protein. (A) Western blot results of comp. (12), transfected group via β-catenin siRNA complexed with f-MWCNTs (12), CNT-TWN, (3) transfected group via β-catenin siRNA complexed with CNT-TWN, lipofectamine, and transfected group via β-catenin siRNA complexed with lipofectamine. (B) the β-catenin protein expression was significantly decreased in β-catenin siRNA complexed with lipofectamine and f-MWCNTs (12) compared with control. ♠Pv<0.05 compared to the control. ♦Pv<0.05 compared to the some species. And all the data were analyzed by a one-way ANOVA test

3.5 Cell viability assay

3.5.1 Effect of beta-catenin knockdown by Lipofectamine or MWCNTs compounds on cell viability.

Cell proliferation and growth were examined using the MTS assay using the Caco-2 cell line. After transfection of β-catenin siRNA by Lipofectamine, *f*-MWCNTs (8), and *f*-MWCNTs (12) in Caco-2 cells as explained previously. All transfection approaches have restricted cell growth significantly. The transfected group via β-catenin siRNA complexed with lipofectamine prevented cell growth and proliferation by 16%, the transfected group via β-catenin siRNA complexed with *f*-MWCNTs (8) prevented cell growth and proliferation by 10%, and the transfected group via β-catenin siRNA

complexed *f*-MWCNTs (12) prevents cell growth and proliferation by 32%. Taking advantage of the cancer cells which can over-express the mannose receptors on their surface, functionalization of CNTs with mannose sugar has a prestigious effect on β-catenin siRNA transfection, consequently, the expression of the β-catenin protein which affects the colorectal cancer cell growth and proliferation.

Figure 3.F

Anti-proliferative effcts of *β-catenin knocdown by siRNA-complexed with f-MWCNTs*

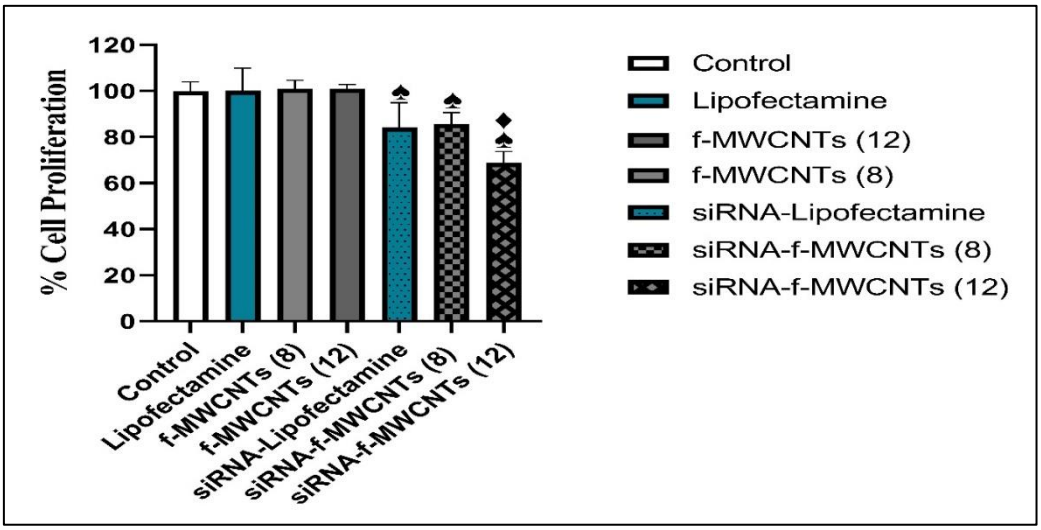

Illustrate the effect of β-catenin knockdown on the growth and proliferation of colorectal cancer cells Caco-2 cells. β-catenin siRNA transfected via lipofectamine, f-MWCNTs (8), and f-MWCNTs (12). Control (Caco-2 cells without transfection), lipofectamine without siRNA, f-MWCNTs (8) without siRNA, f-MWCNTs (12) without siRNA. ♠Pv<0.05 compared to the controls. ♦Pv<0.05 compared to the some species. And all the data were analyzed by a one-way ANOVA test

3.2.2 Effect of beta-catenin knockdawn on the cytotoxicity of 5-FU.

Previously, a few studies were conducted to assess the effect of 5-FU on Caco-2 cells. For instance, Chen et al. assessed the sensitivity of resistant gastric cancer cells to 5-FU after the knockdown of the beta-catenin protein, and at the end of the study they got a promising result, their approach can increase the chemosensitivity of the caco-2 cells to 5-FU [116].

Also, other researchers targeted a signaling pathway that manipulates, certain tumor growth factor (EGF) to induce Caco-2 cells to enter the cell cycle from G0, the results showed that this approach improved the chemosensitivity of Caco-2 cells to 5-FU, up to approximately three times greater sensitivity compared to 5-FU alone [108].

Furthermore, through its role in inhibiting proliferation or inducing programmed cell death, p53 plays a crucial role in the cellular stress response. As well as determining the cellular sensitivity to 5-FU, p53 plays a major role in the anti-cancer effect of 5-FU [84, 86, 87].

Regarding the molecular mechanism of5-FU, the drug can increase the translation, stability, and intensity of P53 activity. Also, the P53 target gene is able to stimulate several tumor suppression processes such as apoptosis, cell cycle arrest, and the sensitivity of colorectal cancer to 5-FU [88]**.** A growing body of information indicates that p53 plays additional roles in a variety of biological processes when it cooperates with other signaling pathways.

Several studies show that p53 has a role in regulating the death of cancer cells as well as their survival via activating of the Wnt pathway, which means that while the drug kills cells by activation of P53, it also promotes their growth [89, 90]. Cancer stem cells (CSCs) play an important role in the clinical benefits of chemotherapy [91].

These cells undergo an endless cycle of self-renewal and differentiation, resulting in the formation of tumor-initiating cells. As a consequence, CSCs allow chemotherapy-treated tumors to relapse [92]. CSC markers have been reported to be associated with poor overall survival after chemotherapy in advanced CRC patients [93, 94]. Furthermore, emerging evidence suggests CSC eradication can contribute to overcoming chemotherapy failure by preventing tumor recurrences through the eradication of CSCs enriched by 5-FU-based therapies [95-97].

Yong-Hee Cho and a co-worker demonstrate that activation of CSCs by 5-FU can induce the transcription factor of the WNT/β-catenin pathway in the colorectal cancer cell line, so combination therapy between 5-FU and Wnt inhibitors can prevent cancer cell growth and prevent disease relapse and recurrence [98]. To investigate the anti-cancer activity of 5-FU in colorectal cancer cell line Caco-2 cell, we treated the cells with 5-FU after they had been transfected by β-catenin siRNA via lipofectamine, *f*-MWCNTs (8), and *f*-MWCNTs (12).

The cell viability was assessed by the MTS assay. The results show that the knockdown of β-catenin has increased the efficacy of 5-FU in the three transfection approaches in

comparison to the control, as we see in figure 3.G (A), (B), and (C). Moreover, the results revealed that 5-FU's cytotoxicity after transfection with *f*-MWCNTs (8)-siRNA is a bit more with an IC50 equal to 66.48 μg/ml compared with its cytotoxicity without transfection (IC50 = 70.01 μg/ml). While 5-FU showed massive destruction of Caco-2 cells after transfection with *f*-MWCNTs-siRNA.

In other words, 5-FU's cytotoxicity increased four times with an IC50 equal to 19.32 μg/ml compared to the control. Also, in the comparison of 500 mcg/ml of 5-FU in each transfection approach, the transfection via *f*-MWCNTs (12)-siRNA had the biggest effect on enhancing the efficacy of the 5-FU 4x greater than with 5-FU without transfection, 3x more than with *f*-MWCNTs (8)-siRNA, and 2.5x in comparison with lipofectamine-siRNA at the same concentration of the drug . *Also, f*-MWCNTs (8) caused an increase in 5-FU efficacy comparable with 5-FU alone, figure 3.G (D).

Furthermore, overexpression of mannose receptors on the surface of Caco-2 cells enhanced the amount of transfected siRNA as well as 5-FU efficacy as seen in f-MWCNTs (12). This implies that the functionalization of CNTs with mannose molecules is crucial to the siRNA transfection process as well as to the solubility, dispersibility, and biocompatibility of the CNTs. The combination therapy of WNT/β-catenin signaling inhibitors and 5-FU exerted a synergistic effect to increase the cellular stress of cancer cells. This resulted in the inhibition of cell proliferation, the inducement of cell death, and increased 5-FU sensitivity.

Therefore, the down-regulation of β-catenin is chemo-sensitizing 5-FU efficacy. Compared with other literature, our approach is more efficient at improving the efficacy of the 5-FU and the chemosensitivity of Caco-2 cells to the 5-FU. So, our approach can be used in colorectal cancer treatment and prevention. Furthermore, we can hypothesize that our compound prevents colorectal cancer recurrence and relapse.

Figure 3.G

5-Fu cytotoxicity after transfection with siRNA-f-MWCNTs

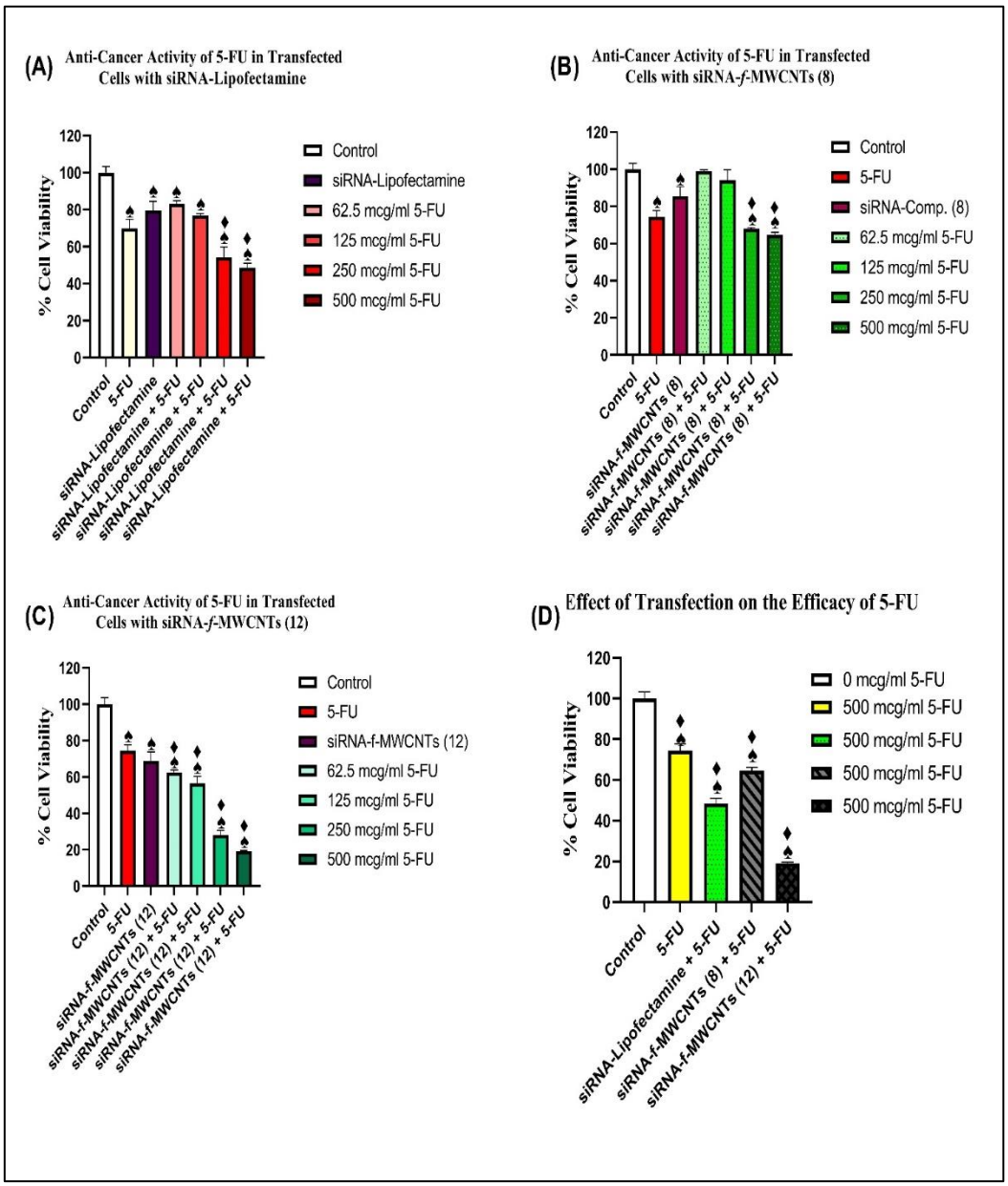

The anti-cancer activity of 5-FU in (A) Caco 2 cells transfected via β-catenin siRNA complexed with lipofectamine, (B) Caco 2 cells transfected via β-catenin siRNA complexed with f-MWCNTs (8), (C) Caco 2 cells transfected via β-catenin siRNA complexed with f-MWCNTs (12), and (D) comparing the anti-cancer activity of the 5-FU in the different approaches at 500 mcg/ml of 5-FU. ♠Pv<0.05 compared to the control. ♦Pv<0.05 compared to some species. And all the data were analyzed by a one-way ANOVA test

3.6 Summary and Conclusion

The chemical synthesis methodology described in this thesis was appropriate for a successful functionalization of the MWCNTs with a tetraamine linker and mannose sugar. In addition, the amount of amine in *f*-MWCNTs (8) was 12.7 * 103 nmol/mg and 40 * 103 nmol/mg in *f*-MWCNTs (12), while the amount of loaded mannose sugar was 20.02 μg/mg in *f*-MWCNTs (12), confirmed by the anthrone method.

The TEM image showed that both types of functionalization with amine and mannose have good dispersibility compared to pristine MWCNTs. In addition, the tetraamine linker in our MWCNTs compounds was able to form a complex with siRNA specific to β-catenin which was proved via gel electrophoresis.

The optimal N/P ratio that can trap β -catenin siRNA starts at 5/1 for the *f*-MWCNTs (8), and 15/1 for the *f*-MWCNTs (12), which was confirmed by gel electrophoresis. Western blot results showed that our compounds were able to decrease the β-catenin protein expression significantly compared with the positive control (lipofectamine). The knockdown percentage was 20% in *f*-MWCNTs (8) and 50% in *f*-MWCNTs (12) while functionalization of MWCNTs with Tween 20 caused an increase in our compound's dispersibility without affecting siRNA transfection. Up-regulation of mannose receptors on the surface of Caco-2 cells causes an increase in the transfection amount of *f*-MWCNTs (12)-siRNA compared with *f*-MWCNTs (8)-siRNA.

The MTS results showed that the down-regulation of β-catenin protein can restrict cell growth and proliferation significantly compared to the control, also this effect can increase the efficacy of 5-FU in colorectal cancer cells, so our approach can be used as adjuvant therapy in colon cancer treatment, and we also hypothesize that our compound is able to prevent colorectal cancer recurrence and relapse.

List of abbreviations

Abbreviation	Meaning
Caco-2 cells	Human colorectal adenocarcinoma
Anhydrous $CuSO_4$	Anhydrous copper sulfate
$CDCl_3$	Deuterochloroform
CGM	Culture growth medium
$CHCl_3$	Chloroform
CNTs	Carbon nanotubes
DCM	Dichloromethane
DDs	Drug delivery systems
DMF	Dimethylformamide
DMSO	Dimethylsulfoxide
DNA	Deoxyribonucleic acid
DOX	Doxorubicin
EDC	Ethylcarbodiimide hydrochloride
EDTA	Ethylene diamine tetra acetic acid
Et_3N	Trimethylamine
FBS	Fetal bovine serum
Hr/s	Hour or Hours
H_2	Hydrogen gas
H_2O	Water
HCl	Hydrochloride
HepG-2	Hepatocellular carcinoma
MCF-7	Human breast cancer cell line
MeOH	Methanol
Min	Minutes
MTS	(3-(4,5-dimethylthiazol-2-yl)-5-(3-carboxymethoxyphenyl)-2-(4-sulfophenyl)-2H-tetrazolium)
MW	Molecular weight
^{o}C	Degree Celsius
o-DCB	Ortho dichlorobenzene
PB	Phosphate buffer
PBS	Phosphate buffer saline
Pd/C	Palladium on carbon
PEG	Polyethylene-glycol
pH	Potential of hydrogen
MWCNTs	Multi-walled Carbon Nanotubes
f-MWCNTs	Functionalized Multi-walled Carbon Nanotubes
RNA	Ribonucleic acid
siRNA	Small interfering Ribonucleic acid
RPMI	Roswell Park Memorial Institute
SWCNT	Single-walled Carbon Nanotube
TEG	Tetraethylene glycol
TEM	Transmission electron microscope
TFA	Trifluoroacetic acid
TGA	Thermogravimetric analysis
THF	Tetrahydrofuran

TLC	Thin layer chromatography
UV-Vis	Ultraviolet-Visible
sRNAs	Small Regulatory RNAs
RPoS	Retail Point of Sale
PGE2	Prostaglandin E2
CSCs	Cancer Stem Cells
TERT	Telomerase reverse transcriptase
XIAP	X-linked inhibitor of apoptosis protein
MMP-9	Matrix metalloproteinase
VEGF	Vascular Endothelial Growth Factor
bFGF	basic Fibroblast Growth Factor
STAT-3	Signal transducers and activators of transcription 3
HSP27	Heat shock protein
λ_{max}	Lambda max

References

1. Maley, C.C., et al., *Classifying the evolutionary and ecological features of neoplasms.* Nat Rev Cancer, 2017. **17**(10): p. 605-619.

2. (WHO), W.H.O. *Cancer* 2018 [cited 2022 27/4]; Available from: https://www.who.int/health-topics/cancer#tab=tab_1.

3. Institute, N.C. *Review: What Is Cancer?* 2022 [cited 2022 4/7]; Available from: https://training.seer.cancer.gov/disease/cancer/review.html.

4. Ribatti, D., *Judah Folkman, a pioneer in the study of angiogenesis.* Angiogenesis, 2008. **11**(1): p. 3-10.

5. Viallard, C. and B. Larrivée, *Tumor angiogenesis and vascular normalization: alternative therapeutic targets.* Angiogenesis, 2017. **20**(4): p. 409-426.

6. Poli, V., L. Seclì, and L. Avalle, *The Microrna-143/145 Cluster in Tumors: A Matter of Where and When.* Cancers (Basel), 2020. **12**(3).

7. Hammond, W.A., A. Swaika, and K. Mody, *Pharmacologic resistance in colorectal cancer: a review.* Therapeutic advances in medical oncology, 2016. **8**(1): p. 57-84.

8. Liu, Y., et al., *Photothermal therapy and photoacoustic imaging via nanotheranostics in fighting cancer.* Chem Soc Rev, 2019. **48**(7): p. 2053-2108.

9. Morrison, A.H., K.T. Byrne, and R.H. Vonderheide, *Immunotherapy and Prevention of Pancreatic Cancer.* Trends Cancer, 2018. **4**(6): p. 418-428.

10. Sun, J., et al., *Clinical significance of palliative gastrectomy on the survival of patients with incurable advanced gastric cancer: a systematic review and meta-analysis.* BMC Cancer, 2013. **13**: p. 577.

11. Goh, I., O. Lai, and L. Chew, *Prevalence and Risk of Polypharmacy Among Elderly Cancer Patients Receiving Chemotherapy in Ambulatory Oncology Setting.* Curr Oncol Rep, 2018. **20**(5): p. 38.

12. Hackenberg, M., et al., *Generation of different sizes and classes of small RNAs in barley is locus, chromosome and/or cultivar-dependent.* BMC genomics, 2016. **17**(1): p. 1-11.

13. Lumencandela. *RNA-Based Regulation.* [cited 2022 7/4]; Available from: https://courses.lumenlearning.com/boundless-microbiology/chapter/rna-based-regulation/.

14. Yadav, S., et al., *Natural and artificial small RNAs: a promising avenue of nucleic acid therapeutics for cancer.* Cancer Biol Med, 2017. **14**(3): p. 242-253.

15. Mendonça, L., M. Pedroso de Lima, and S. Simões, *Targeted lipid-based systems for siRNA delivery.* Journal of Drug Delivery Science and Technology, 2012. **22**: p. 65-73.

16. Goessling, W., et al., *Genetic interaction of PGE2 and Wnt signaling regulates developmental specification of stem cells and regeneration.* Cell, 2009. **136**(6): p. 1136-47.

17. Cohen, E.D., et al., *Wnt/β-catenin signaling promotes expansion of Isl-1–positive cardiac progenitor cells through regulation of FGF signaling.* The Journal of clinical investigation, 2007. **117**(7): p. 1794-1804.

18. Zeng, X., et al., *Initiation of Wnt signaling: control of Wnt coreceptor Lrp6 phosphorylation/activation via frizzled, dishevelled and axin functions.* 2008.

19. Eastman, Q. and R. Grosschedl, *Regulation of LEF-1/TCF transcription factors by Wnt and other signals.* Current opinion in cell biology, 1999. **11**(2): p. 233-240.

20. Huber, O., et al., *Nuclear localization of β-catenin by interaction with transcription factor LEF-1.* Mechanisms of development, 1996. **59**(1): p. 3-10.

21. Nelson, W.J. and R. Nusse, *Convergence of Wnt, ß-catenin, and cadherin pathways.* Science, 2004. **303**(5663): p. 1483-1487.

22. Bullions, L.C. and A.J. Levine, *The role of beta-catenin in cell adhesion, signal transduction, and cancer.* Current opinion in oncology, 1998. **10**(1): p. 81-87.

23. Kléber, M. and L. Sommer, *Wnt signaling and the regulation of stem cell function.* Current opinion in cell biology, 2004. **16**(6): p. 681-687.

24. Li, L., Y. Wei, and C. Gong, *Polymeric nanocarriers for non-viral gene delivery.* Journal of Biomedical Nanotechnology, 2015. **11**(5): p. 739-770.

25. Gardlík, R., et al., *Vectors and delivery systems in gene therapy.* Med Sci Monit, 2005. **11**(4): p. 110-121.

26. Huang, S. and M. Kamihira, *Development of hybrid viral vectors for gene therapy.* Biotechnology advances, 2013. **31**(2): p. 208-223.

27. Nayerossadat, N., T. Maedeh, and P.A. Ali, *Viral and nonviral delivery systems for gene delivery.* Advanced biomedical research, 2012. **1**(1): p. 27.

28. Oehmig, A., et al., *Herpes simplex virus type 1 amplicons and their hybrid virus partners, EBV, AAV, and retrovirus.* Current Gene Therapy, 2004. **4**(4): p. 385-408.

29. Chellappan, D.K., et al., *Gene therapy and type 1 diabetes mellitus.* Biomedicine & Pharmacotherapy, 2018. **108**: p. 1188-1200.

30. Elhissi, A., *Liposomes for pulmonary drug delivery: the role of formulation and inhalation device design.* Current pharmaceutical design, 2017. **23**(3): p. 362-372.

31. Mukherjee, A., et al., *Lipid–polymer hybrid nanoparticles as a next-generation drug delivery platform: state of the art, emerging technologies, and perspectives.* International journal of nanomedicine, 2019. **14**: p. 1937.

32. Salkho, N., et al., *Liposomes as a promising ultrasound-triggered drug delivery system in cancer treatment.* Current molecular medicine, 2017. **17**(10): p. 668-688.

33. Shah, S., et al., *Liposomes: Advancements and innovation in the manufacturing process.* Advanced Drug Delivery Reviews, 2020. **154**: p. 102-122.

34. Elsana, H., et al., *Evaluation of novel cationic gene based liposomes with cyclodextrin prepared by thin film hydration and microfluidic systems.* Scientific reports, 2019. **9**(1): p. 1-17.

35. Do, H.D., et al., *Development of theranostic cationic liposomes designed for image-guided delivery of nucleic acid.* Pharmaceutics, 2020. **12**(9): p. 854.

36. Liu, C., et al., *Barriers and strategies of cationic liposomes for cancer gene therapy.* Molecular Therapy-Methods & Clinical Development, 2020. **18**: p. 751-764.

37. Cardarelli, F., et al., *The intracellular trafficking mechanism of Lipofectamine-based transfection reagents and its implication for gene delivery.* Scientific reports, 2016. **6**(1): p. 1-8.

38. Wang, T., et al., *Systematic screening of commonly used commercial transfection reagents towards efficient transfection of single-stranded oligonucleotides.* Molecules, 2018. **23**(10): p. 2564.

39. Inglut, C.T., et al., *Immunological and Toxicological Considerations for the Design of Liposomes.* Nanomaterials (Basel), 2020. **10**(2).

40. Bozzuto, G. and A. Molinari, *Liposomes as nanomedical devices.* Int J Nanomedicine, 2015. **10**: p. 975-99.

41. Logothetidis, S., *Nanomedicine: the medicine of tomorrow*, in *Nanomedicine and Nanobiotechnology*. 2012, Springer. p. 1-26.

42. Freitas Jr, R.A., *What is nanomedicine?* Nanomedicine: Nanotechnology, Biology and Medicine, 2005. **1**(1): p. 2-9.

43. Abeer, S., *Future medicine: nanomedicine.* Jimsa, 2012. **25**(3): p. 187-192.

44. Satalkar, P., B.S. Elger, and D.M. Shaw, *Defining nano, nanotechnology and nanomedicine: why should it matter?* Science and engineering ethics, 2016. **22**(5): p. 1255-1276.

45. Dresselhaus, G., M.S. Dresselhaus, and R. Saito, *Physical properties of carbon nanotubes*. 1998: World scientific.

46. Popov, V.N., *Carbon nanotubes: properties and application.* Materials Science and Engineering: R: Reports, 2004. **43**(3): p. 61-102.

47. Rathinavel, S., K. Priyadharshini, and D. Panda, *A review on carbon nanotube: An overview of synthesis, properties, functionalization, characterization, and the application.* Materials Science and Engineering: B, 2021. **268**: p. 115095.

48. Reich, S., C. Thomsen, and J. Maultzsch, *Carbon nanotubes: basic concepts and physical properties*. 2004: John Wiley & Sons.

49. Salvetat, J.-P., et al., *Mechanical properties of carbon nanotubes.* Applied Physics A, 1999. **69**(3): p. 255-260.

50. Shoukat, R. and M.I. Khan, *Carbon nanotubes: A review on properties, synthesis methods and applications in micro and nanotechnology.* Microsystem Technologies, 2021. **27**(12): p. 4183-4192.

51. Sun, Y.-P., et al., *Functionalized carbon nanotubes: properties and applications.* Accounts of chemical research, 2002. **35**(12): p. 1096-1104.

52. Yakovenko, O.S., et al., *Electromagnetic properties of carbon nanotube/BaFe12−xGaxO19/Epoxy composites with random and oriented filler distributions.* Nanomaterials, 2021. **11**(11): p. 2873.

53. Ribeiro, B., et al., *Carbon nanotube buckypaper reinforced polymer composites: a review.* Polímeros, 2017. **27**: p. 247-255.

54. Eatemadi, A., et al., *Carbon nanotubes: properties, synthesis, purification, and medical applications.* Nanoscale research letters, 2014. **9**(1): p. 1-13.

55. Sadrolhosseini, A.R., et al., *Laser ablation technique for synthesis of metal nanoparticle in liquid.* Laser Technology and its Applications, 2018: p. 63-81.

56. Liu, Z., et al., *Carbon nanotubes in biology and medicine: in vitro and in vivo detection, imaging and drug delivery.* Nano research, 2009. **2**(2): p. 85-120.

57. Malarkey, E.B. and V. Parpura, *Carbon nanotubes in neuroscience.* Acta Neurochir Suppl, 2010. **106**: p. 337-41.

58. Ando, Y., et al., *Growing carbon nanotubes.* Materials today, 2004. **7**(10): p. 22-29.

59. Malarkey, E.B. and V. Parpura, *Carbon nanotubes in neuroscience.* Brain edema XIV, 2010: p. 337-341.

60. Raphey, V., et al., *Advanced biomedical applications of carbon nanotube.* Materials Science and Engineering: C, 2019. **100**: p. 616-630.

61. Rode, A., S. Sharma, and D.K. Mishra, *Carbon nanotubes: classification, method of preparation and pharmaceutical application.* Current drug delivery, 2018. **15**(5): p. 620-629.

62. Madani, S.Y., A. Mandel, and A.M. Seifalian, *A concise review of carbon nanotube's toxicology.* Nano Rev, 2013. **4**.

63. Zhang, C., et al., *Carbon Nanotubes: A Summary of Beneficial and Dangerous Aspects of an Increasingly Popular Group of Nanomaterials.* Front Oncol, 2021. **11**: p. 693814.

64. Ge, C., et al., *The contributions of metal impurities and tube structure to the toxicity of carbon nanotube materials.* NPG Asia Materials, 2012. **4**(12): p. e32-e32.

65. Mohanta, D., et al., *Carbon nanotubes: Evaluation of toxicity at biointerfaces.* J Pharm Anal, 2019. **9**(5): p. 293-300.

66. Francis, A.P. and T. Devasena, *Toxicity of carbon nanotubes: A review.* Toxicology and industrial health, 2018. **34**(3): p. 200-210.

67. Xie, G., et al., *Graphene-based materials for hydrogen generation from light-driven water splitting.* Advanced materials, 2013. **25**(28): p. 3820-3839.

68. Horibata, K., et al., *In vivo genotoxicity assessment of a multiwalled carbon nanotube in a mouse ex vivo culture.* Genes Environ, 2022. **44**(1): p. 24.

69. Liang, G., et al., *Preparation and biodistribution of tyrosine modified multiwall carbon nanotubes.* J Nanosci Nanotechnol, 2010. **10**(12): p. 8508-15.

70. Saleemi, M.A., et al., *Toxicity of Carbon Nanotubes: Molecular Mechanisms, Signaling Cascades, and Remedies in Biomedical Applications.* Chem Res Toxicol, 2021. **34**(1): p. 24-46.

71. Zaib, Q. and F. Ahmad, *Optimization of Carbon Nanotube Dispersions in Water Using Response Surface Methodology.* ACS Omega, 2019. **4**(1): p. 849-859.

72. Saka, C., *Overview on the surface functionalization mechanism and determination of surface functional groups of plasma treated carbon nanotubes.* Critical Reviews in Analytical Chemistry, 2018. **48**(1): p. 1-14.

73. Yeo, E.S., et al., *Functionalization and dispersion of carbon nanomaterials using an environmentally friendly ultrasonicated ozonolysis process.* JoVE (Journal of Visualized Experiments), 2017(123): p. e55614.

74. Angelikopoulos, P., et al., *Dispersing individual single-wall carbon nanotubes in aqueous surfactant solutions below the cmc.* The Journal of Physical Chemistry C, 2010. **114**(1): p. 2-9.

75. Debnath, S., et al., *A study of the interaction between single-walled carbon nanotubes and polycyclic aromatic hydrocarbons: toward structure− property relationships.* The Journal of Physical Chemistry C, 2008. **112**(28): p. 10418-10422.

76. Gao, J., et al., *Selective wrapping and supramolecular structures of polyfluorene–carbon nanotube hybrids.* ACS nano, 2011. **5**(5): p. 3993-3999.

77. Zhao, Y.-L. and J.F. Stoddart, *Noncovalent functionalization of single-walled carbon nanotubes.* Accounts of chemical research, 2009. **42**(8): p. 1161-1171.

78. Yang, K., L. Zhu, and B. Xing, *Adsorption of polycyclic aromatic hydrocarbons by carbon nanomaterials.* Environmental science & technology, 2006. **40**(6): p. 1855-1861.

79. Kushwaha, S.K.S., et al., *Carbon nanotubes as a novel drug delivery system for anticancer therapy: a review.* Brazilian Journal of Pharmaceutical Sciences, 2013. **49**: p. 629-643.

80. Tagmatarchis, N. and M. Prato, *Functionalization of carbon nanotubes via 1, 3-dipolar cycloadditions.* Journal of materials chemistry, 2004. **14**(4): p. 437-439.

81. Tandon, H., et al., *A review of a computational study of carbon nanotubes.* Carbon Nanotubes and Nanoparticles, 2019: p. 25-38.

82. Zamolo, V.A., E. Vazquez, and M. Prato, *Carbon nanotubes: synthesis, structure, functionalization, and characterization.* Polyarenes II, 2013: p. 65-109.

83. Longley, D.B., D.P. Harkin, and P.G. Johnston, *5-Fluorouracil: mechanisms of action and clinical strategies.* Nature Reviews Cancer, 2003. **3**(5): p. 330-338.

84. Zhang, N., et al., *5-Fluorouracil: mechanisms of resistance and reversal strategies.* Molecules, 2008. **13**(8): p. 1551-69.

85. Vodenkova, S., et al., *5-fluorouracil and other fluoropyrimidines in colorectal cancer: Past, present and future.* Pharmacol Ther, 2020. **206**: p. 107447.

86. Hafner, A., et al., *The multiple mechanisms that regulate p53 activity and cell fate.* Nat Rev Mol Cell Biol, 2019. **20**(4): p. 199-210.

87. Longley, D.B., D.P. Harkin, and P.G. Johnston, *5-fluorouracil: mechanisms of action and clinical strategies.* Nat Rev Cancer, 2003. **3**(5): p. 330-8.

88. Ju, J., et al., *Regulation of p53 expression in response to 5-fluorouracil in human cancer RKO cells.* Clin Cancer Res, 2007. **13**(14): p. 4245-51.

89. Lee, K.H., et al., *A genomewide study identifies the Wnt signaling pathway as a major target of p53 in murine embryonic stem cells.* Proc Natl Acad Sci U S A, 2010. **107**(1): p. 69-74.

90. Wang, Q., et al., *The p53 Family Coordinates Wnt and Nodal Inputs in Mesendodermal Differentiation of Embryonic Stem Cells.* Cell Stem Cell, 2017. **20**(1): p. 70-86.

91. Dean, M., T. Fojo, and S. Bates, *Tumour stem cells and drug resistance.* Nat Rev Cancer, 2005. **5**(4): p. 275-84.

92. Marusyk, A., V. Almendro, and K. Polyak, *Intra-tumour heterogeneity: a looking glass for cancer?* Nat Rev Cancer, 2012. **12**(5): p. 323-34.

93. Eppert, K., et al., *Stem cell gene expression programs influence clinical outcome in human leukemia.* Nat Med, 2011. **17**(9): p. 1086-93.

94. Sadanandam, A., et al., *A colorectal cancer classification system that associates cellular phenotype and responses to therapy.* Nat Med, 2013. **19**(5): p. 619-25.

95. Dahan, P., et al., *Ionizing radiations sustain glioblastoma cell dedifferentiation to a stem-like phenotype through survivin: possible involvement in radioresistance.* Cell Death Dis, 2014. **5**(11): p. e1543.

96. Giuliano, M., et al., *Circulating tumor cells as prognostic and predictive markers in metastatic breast cancer patients receiving first-line systemic treatment.* Breast Cancer Res, 2011. **13**(3): p. R67.

97. Pierga, J.Y., et al., *High independent prognostic and predictive value of circulating tumor cells compared with serum tumor markers in a large prospective trial in first-line chemotherapy for metastatic breast cancer patients.* Ann Oncol, 2012. **23**(3): p. 618-624.

98. Cho, Y.H., et al., *5-FU promotes stemness of colorectal cancer via p53-mediated WNT/β-catenin pathway activation.* Nat Commun, 2020. **11**(1): p. 5321.

99. Mai, Y.-J., et al., *Effects of beta-catenin-specific siRNA interference on Jurkat and K562 cells.* Zhongguo yi xue ke xue Yuan xue bao. Acta Academiae Medicinae Sinicae, 2008. **30**(3): p. 290-295.

100. Li, K., et al., *Knockdown of β-catenin by siRNA influences proliferation, apoptosis and invasion of the colon cancer cell line SW480.* Oncology letters, 2016. **11**(6): p. 3896-3900.

101. Teng, Y., et al., *Effect of siRNA-mediated beta-catenin gene on Wnt signal pathway in lung adenocarcinoma A549 cell.* Zhonghua yi xue za zhi, 2010. **90**(14): p. 988-992.

102. Yu, F., et al., *The study of siRNA interference after laryngeal cancer Hep-2 cells to cisplatin sensitivity of β-catenin gene expression.* Lin Chuang er bi yan hou tou Jing wai ke za zhi= Journal of Clinical Otorhinolaryngology, Head, and Neck Surgery, 2015. **29**(13): p. 1143-1147.

103. Liyan, W., S. Xun, and M. Xiangwei, *Effect of β-catenin siRNA on proliferation and apoptosis of hepatoma cell line SMMC-7721 and HepG-2.* Hepato-gastroenterology, 2011. **58**(110-111): p. 1757-1764.

104. Wang, X.-H., et al., *β-catenin siRNA regulation of apoptosis-and angiogenesis-related gene expression in hepatocellular carcinoma cells: potential uses for gene therapy.* Oncology reports, 2010. **24**(4): p. 1093-1099.

105. Zhang, J.-G., et al., *Effect of siRNA-interfering β-catenin expression on MDR of human multiple myeloma cell line.* Zhongguo shi yan xue ye xue za zhi, 2019. **27**(2): p. 477-481.

106. Chen, W., et al., *Construction of Aptamer-siRNA Chimera/PEI/5-FU/Carbon Nanotube/Collagen Membranes for the Treatment of Peritoneal Dissemination of Drug-Resistant Gastric Cancer.* Advanced Healthcare Materials, 2020. **9**(21): p. 2001153.

107. Niu, Q., et al., *Construction of Durvalumab/carbon nanotube/PEI/aptamer-siRNA chimera for the immunotherapy of hepatocellular carcinoma.* Biomed Mater, 2022.

108. Ye, L., et al., *Reduction of G0 phase cells of colon cancer caco-2 cells may enhance 5-fluorouracil efficacy.* J Biomed Res, 2010. **24**(1): p. 64-8.

109. Jarre, G., et al., *Synthesis of nanodiamond derivatives carrying amino functions and quantification by a modified Kaiser test.* Beilstein journal of organic chemistry, 2014. **10**(1): p. 2729-2737.

110. Roe, J.H., *The determination of dextran in blood and urine with anthrone reagent.* J Biol Chem, 1954. **208**(2): p. 889-896.

111. Scott Jr, T.A. and E.H. Melvin, *Determination of dextran with anthrone.* Analytical Chemistry, 1953. **25**(11): p. 1656-1661.

112. Assali, M., et al., *Covalent functionalization of graphene sheets for plasmid DNA delivery: experimental and theoretical study.* RSC Adv, 2023. **13**(10): p. 7000-7008.

113. Assali, M., et al., *Dual covalent functionalization of single-walled carbon nanotubes for effective targeted cancer therapy.* Nanotechnology, 2021. **32**(20): p. 205101.

114. Couce, M.E., A.J. Weatherington, and J.F. McGINTY, *Expression of insulin-like growth factor-II (IGF-II) and IGF-II/mannose-6-phosphate receptor in the rat hippocampus: an in situ hybridization and immunocytochemical study.* Endocrinology, 1992. **131**(4): p. 1636-1642.

115. System, P. *Atomic Force Microscope* 2023 [cited 2023 25/3]; Available from: https://www.parksystems.com/products/small-sample-afm/park-nx10/overview?utm_source=google&utm_medium=cpc&utm_campaign=NX10-eu-070822-keyword&gclid=CjwKCAjw_YShBhAiEiwAMomsEGRNJBShJ9RLYrG1Xm74HSdg67JN8OQDK0zeA0GBb6yS52o4INSabRoCqyUQAvD_BwE.

116. Chen, W., et al., *Construction of Aptamer-siRNA Chimera/PEI/5-FU/Carbon Nanotube/Collagen Membranes for the Treatment of Peritoneal Dissemination of Drug-Resistant Gastric Cancer.* Adv Healthc Mater, 2020. **9**(21): p. e2001153.

جامعة النجاح الوطنية

كلية الدراسات العليا

تثبيط البيتا كاتينين في الخلايا السرطانية بواسطة الحمض الرايبوزومي القصير المتداخل المحمل على أنابيب الكاربون النانوية

إعداد

أحمد غريب

إشراف

د. نعيم كتانة

د. محي الدين العسالي

قدمت هذه الرسالة استكمالا لمتطلبات الحصول على درجة الماجستير في علم الأدوية، من كلية الدراسات العليا، في جامعة النجاح الوطنية، نابلس- فلسطين.

2023

تثبيط البيتا كاتينين في الخلايا السرطانية بواسطة الحمض الرايبوزومي القصير المتداخل المحمل على أنابيب الكاربون النانوية

إعداد

أحمد غريب

إشراف

د. نعيم كتانة

د. محي الدين العسالي

الملخص

على الصعيد العالمي، وفقاً لمنظمة الصحة العالمية يعد مرض السرطان ثاني سبب للوفاة في جميع أنحاء العالم، من أجل السيطرة على مرض السرطان، تم استخدام العديد من الاستراتيجيات مثل: الجراحة، الإشعاع، العلاج الكيماوي والعلاج الجيني.

استفادت أبحاث الطب من العلاج القائم على التكنولوجيا الحيوية في السنوات العديدة الماضية، وكواحدة من أحدث الاستراتيجيات في علاج السرطان، مثل استخدام الحمض الرايبوزومي القصير المتداخل للتحكم في التعبير الجيني، ومع ذلك، توصيل الحمض الرايبوزومي القصير المتداخل لخلايا السرطان يمثل تحدياً، لا سيما أثناء الفحوصات على الكائنات الحية.

حالياً يتم استخدام مركب اللايبوفيكتامين لهذا الهدف، ولكن لسوء الحظ، أظهر المركب سمية غير مقبولة في الكائنات الحية. لإيصال هذه الأنواع من الجزيئات دون التسبب في ضرر كبير، يعمل الباحثون على تطوير أنظمة توصيل تكنولوجية جديدة. لقد حظي تطوير أنظمة توصيل الأدوية القائمة على أنابيب الكاربون النانونية بالكثير من الاهتمام في هذا المجال.

يهدف مشروعنا إلى تطوير طريقة جديدة لإيصال الحمض الرايبوزومي القصير المتداخل الى خلايا سرطان القولون لاستهداف ترجمة بروتين البيتا-كاتينين المعروف أن له دوراً في العديد من عمليات

التطور، بما في ذلك نمو الخلايا وتكاثرها، والتكوينات الجنينية، وتمايز الخلايا، وغيرها من الوظائف الخلوية.

تعتمد الاستراتيجية الجديدة على تصنيع نظام نانوني جديد من أنابيب الكربون النانونية متعددة الجدران ا لمفعل بواسطة مركب رباعي الأمين وسكر المانوز كعامل استهداف لزيادة دخول المركب النانوني وانتقائيته.

لقد تمكنا من تفعيل أنابيب الكاربون النانونية متعددة الجدران بواسطة مركبات رباعي الأمين مركب 8 ومن ثم تفعيلها بواسطة جزيئات سكر المانوز مركب 12 التي تم تأكيدها بواسطة الفحص المجهري الالكتروني النافذ.

بالإضافة الى ذلك، كمية رباعي الأمين على المركب 8 كانت 12.7 * 10^3 نانومول/ملغم و40 * 10^3 نانومول/ملغم في مركب 12 كما تم تأكيده بطرية الأنثرون.

تبدأ نسبة النيتروجين/فوسفات التي تحبس الحمض الرايبوزومي القصير المتداخل من 5:1 لمركب 8 و15:1 لمركب 12 والذي تم تأكيده بواسطة الفصل الكهربائي الهلامي.

أظهرت نتائج وسترن بلوت أن مركباتنا قادرة على التقليل من تعبير بروتين البيتا-كاتينين بشكل ملحوظ، حيث كانت نسبة تثبيط البروتين 20% لمركب 8 و50% لمركب 12، بينما تفعيل أنابيب الكاربون بواسطة توين 20 أدى الى زيادة فصل المركبات دون التأثير على دخول الحمض الرايبوزومي الى الخلايا.

افترضنا أن زيادة تكون مستقبلات المانوز على سطح خلايا قولون السرطان قد يزيد من عملية نقل دخول الحمض الرايبوزومي القصير المتداخل بواسطة مركب 12.

أظهرت نتائج تكاثر الخلايا أن تثبيط ترجمة بروتين البيتا-كاتينين يمكنه أن يحد من نمو الحمض الرايبوزومي، كما أن هذا التأثير يمكن أن يزيد من فعالية الفلوروبوراسيل الخماسي (5-FU) في سرطان القولون بشكل ملحوظ مقارنه مع المجموعة المرجع، لذلك نقترح أنه يمكن تنفيذ نهجنا في علاج سرطان القولون.

الكلمات المفتاحية: البيتا-كاتينين، سرطان القولون، أنابيب الكربون النانونية متعددة الجدران.